Enclosure 4

Submittal of Comments and Proprietary Markings on the Draft Safety Evaluation for Topical Report WCAP-17794-P/WCAP-17794-NP, Revision 0, "10x10 SVEA Fuel Critical Power Experiments and New CPR Correlation: D5 for SVEA-96 Optima3," (EPID L-2014-TOP-0002)

(Non-Proprietary)

August 2019

Westinghouse Electric Company
1000 Westinghouse Drive
Cranberry Township, PA 16066

Westinghouse has reviewed the NRCs Draft Safety Evaluation (SE) and offers the following comments.

Westinghouse is in agreement with the NRC's suggested proprietary information markings. In addition, we offer the following comments and additional suggested proprietary markings. Westinghouse's suggested changes and proprietary markings are highlighted in the attached mark-up of the draft SE.

	SE Page	**Comment**
1.	11	1st paragraph, add additional proprietary markings.
2.	11	2nd paragraph, next to last line, change to read: "…less than the…"
3.	14	4th paragraph, 2nd line, delete the second occurrence of "or were."
4.	25	In 3.1.3.2.5, items A. through H., add additional proprietary markings.
5.	26	1st (2 places), 2nd, 5th, and 6th paragraphs, add additional proprietary markings.
6.	28	In 3.1.3.3.2, add additional proprietary markings.
7.	31	In 3.1.3.4.2, at the end of the 2nd paragraph, add a closing bracket.
8.	33	In 3.1.3.5.3, 2nd paragraph, 3rd line, change to read: "…limiting transients were…"
9.	34	1st paragraph, last line, change to read: "…on SVEA-96…"
10.	34	In 3.2.1.1, 1st paragraph, next to last line, change "…its power was…" to read: "…the power in a neighboring cell was…"
11.	42	4th full paragraph, start of 4th line, change to read: "Either zero or two vortices could…."
12.	44	Section 4.0, item 2, add additional proprietary markings (2 places).

U. S. NUCLEAR REGULATORY COMMISSION

OFFICE OF NUCLEAR REACTOR REGULATION

DRAFT SAFETY EVALUATION FOR TOPICAL REPORT WCAP-17794-P, REVISION 0, AND WCAP-17794-NP, REVISION 0, "10X10 SVEA FUEL CRITICAL POWER EXPERIMENTS AND NEW CPR CORRELATION: D5 FOR SVEA-96 OPTIMA3"

WESTINGHOUSE ELECTRIC COMPANY

CAC NO. MF3368; EPID: L-2014-TOP-0002

Enclosure

TABLE OF CONTENTS

1.0 INTRODUCTION

By letter dated November 22, 2013 (Ref. 1), Westinghouse Electric Company (WEC or Westinghouse) submitted Topical Report (TR) WCAP-17794-P, Revision 0, and WCAP-17794-NP, Revision 0, "10x10 SVEA Fuel Critical Power Experiments and New CPR [Critical Power Ratio] Correlation: D5 for SVEA-96 Optima3" (Ref. 2), to the U.S. Nuclear Regulatory Commission (NRC) for review and approval. The purpose of this report was to describe the critical power (CP) model for calculating the CPR model for Westinghouse SVEA-96 Optima3 boiling water reactor (BWR) fuel assemblies. The new model is referred to as the D5 model and is based on the experience obtained from the other CPR models of D1 (Ref. 3), D2 (Ref. 4), and D4 (Ref. 5).

The complete list of correspondence between the NRC and Westinghouse is provided in Table 1 below. This includes request for additional information (RAI) questions, responses to RAI questions, audit documentation, and any other correspondence relevant to this review.

Table 1: List of Key Correspondence

Owner	Document	Document Date	Reference
WEC	Submittal Letter	November 22, 2013	1
WEC	Topical Report	November 22, 2013	2
NRC	Acceptance Letter	April 28, 2014	6
NRC	Audit Plan	May 18, 2015	7
NRC	Audit Report	June 18, 2015	8
WEC	Supporting Data	June 18, 2015	9
NRC	RAI – Round 1	May 31, 2016	10
WEC	RAI Responses	August 8, 2016	11
NRC	RAI - Follow-up	November 21, 2016	12
NRC	Audit Plan	March 12, 2017	13
WEC	Audit Supporting Information for RAI	March 16, 2017	14
WEC	Audit Information	April 4, 2017	15
WEC	Audit Follow-up Information	April 13, 2017	16
NRC	RAI - Follow-up	May 15, 2017	17
WEC	RAI Responses	June 12, 2017	18
WEC	RAI Response on Fuel Failure Impact	December 18, 2017	19
WEC	Final RAI Response on Fuel Failure Impact	July 16, 2018	20
WEC	Final Audit Slides	December 19, 2018	21

Additionally, the NRC staff had several RAI questions. General information for each RAI including its number, its topic, its associated goal, and the reference(s) of its response are given in below.

Table 2: Listing of RAIs

RAI	Subject	Associated Goal	Reference of RAI	Reference of Response
RAI-SNPB-01	Reference for Test Facility	G1.1.1, G1.2.1	10	11
RAI-SNPB-02	Validation for Test Facility	G1.1.2	10	11
RAI-SNPB-03	Plots for Range of Parameters	G3.2.3, G3.2.4, G3.2.5	10	11, 14, 18
RAI-SNPB-04	Difference in Dimensions Between Fuel and Test Bundle	G1.3.1	10	11, 14, 18
RAI-SNPB-05	Difference in Grid Spacer Types Between Fuel and Test Bundle	G1.3.2	10	11
RAI-SNPB-06	Axial Shift in Grid Spacers	G1.3.1	10	11, 14, 18
RAI-SNPB-07	Radial Power Distributions	G1.3.4	10	11, 18
RAI-SNPB-08	Axial Power Distributions	G1.3.3	10	11
RAI-SNPB-09	Part Length Fuel Rods	G1.3.1	10	11, 18
RAI-SNPB-10	More Detailed Test Procedures	G1.2.1	10	11
RAI-SNPB-11	Reference for Test Procedures	G1.2.1	10	11
RAI-SNPB-12	Statistical Design of Experiments	G1.2.2	10	11
RAI-SNPB-13	Mass Flux Uncertainty	G1.2.3	10	11
RAI-SNPB-14	Other Means of Measurement	G1.2.4	10	11
RAI-SNPB-15	Instrumentation Calibration	G1.2.5	10	11
RAI-SNPB-16	Calculation of CPR Uncertainty	G1.2.6	10	11
RAI-SNPB-17	Experimental Uncertainty	G1.2.6	10	11, 14, 18
RAI-SNPB-18	Quantified Heat Losses	G1.2.7	10	11, 14, 18
RAI-SNPB-19	Derivation of the Transient Correlation	G2.1.2	10	11
RAI-SNPB-20	I_2 Limits	G2.1.2	10	11, 18
RAI-SNPB-21	Process for Generating Correlation Coefficients	G2.2.2, G2.2.3	10	11
RAI-SNPB-22	MEFISTO Analysis	G2.2.2	10	11
RAI-SNPB-23	Validation Data	G3.4.1	10	11
RAI-SNPB-24	Enforcement of the Computational Domain	G3.2.6	10	11
RAI-SNPB-25	Sparse Region (1) in the Computational Domain	G3.2.5	10	11, 18

RAI-SNPB-26	Sparse Region (1) in the Computational Domain	G3.2.5	10	11
RAI-SNPB-27	Sparse Region (2) in the Computational Domain	G3.2.5	10	11
RAI-SNPB-28	Other Sparse Regions in the Computational Domain	G3.2.5	10	11, 14, 18
RAI-SNPB-29	Demonstrate Data Set Poolability	G3.3.1	10	11, 14, 18
RAI-SNPB-30	Negative Bias	G3.4.2	10	11
RAI-SNPB-31	Figures 4-9 and 4-10	G3.3.2	10	11
RAI-SNPB-32	Degrees of Freedom	G3.4.2	10	11
RAI-SNPB-33	Transient Selection	G3.5.3	10	11, 18
RAI-SNPB-34	BISON-SLAVE	G3.5.1	10	11, 18
RAI-SNPB-35	Figure 7-2	N/A	10	11
RAI-SNPB-36	Dryout	G1.3.5	12	15, 16
RAI-SNPB-37	Data Analysis	G3.3.2	17	14, 18, 20, 21

2.0 REGULATORY EVALUATION

There are four main regulations in Title 10 of the *Code of Federal Regulations* (10 CFR) associated with critical boiling transition (CBT):

- 10 CFR Part 50, Appendix A, Criterion 10
- 10 CFR 50.36
- 10 CFR 50.34
- 10 CFR, Part 50, Appendix B

General Design Criterion (GDC) 10 in 10 CFR Part 50, Appendix A, is the principal regulation associated with a CBT. This criterion introduces the concept of specified acceptable fuel design limits (SAFDLs). SAFDLs are those limits placed on certain variables to ensure that the fuel does not fail. One such SAFDL is associated with CBT. Because the decrease in heat transfer following a CBT could result in fuel failure, a SAFDL is used to demonstrate that a CBT does not occur during normal operation and anticipated operational occurrences (AOOs). Therefore, fuel failure is precluded during normal operation and AOOs.[1]

NUREG-0800, “Standard Review Plan” (SRP), Section 4.4, includes the following two SAFDLs for use in accounting for the uncertainties involved in developing and using a CBT model (e.g., uncertainties in the values of process parameters, core design parameters, calculation methods, instrumentation) and ensuring that fuel failure is precluded:

(a) There should be a 95-percent probability at the 95-percent confidence level that the hot fuel rod in the core does not experience a CBT during normal operation or AOOs.

[1] Experiencing such a transition may not immediately result in fuel failure. The decrease in heat transfer and subsequent increase in fuel temperature may not be enough to cause the cladding to weaken or melt. Therefore, the point of CBT is considered to be a conservative limit compared to the actual point of fuel damage.

(b) At least 99.9 percent of the fuel rods in the core will not experience a CBT during normal operation or AOOs.

Typically, SAFDL (a) is associated with pressurized water reactors (PWRs) and SAFDL (b) is associated with BWRs.

Before May 21, 1971, when the GDC took effect, the Atomic Energy Commission (AEC), the predecessor to the NRC, approved construction permits for nuclear power plants based on plant-specific Principal Design Criteria (PDC) that applicants proposed in their construction permit applications as required by the then-extant provisions of 10 CFR 50.34(a). The AEC published proposed General Design Criteria in the *Federal Register* (32 FR 10213) on July 11, 1967, sometimes referred to as the AEC Draft GDC, which were generally consistent with the PDC previously proposed in applications for construction permits. AEC Draft GDC 6 is the relevant draft GDC which is substantially like the current GDC 10, and also calls for the reactor core to be designed with appropriate margin to specified limits which preclude fuel damage.

The second regulation associated with CBT is 10 CFR 50.36, part of which focuses on defining technical specification (TS) safety limits. There are multiple limits that are associated with CBT models used during plant operation. These limits can be operating limits, alarms, analysis limits, and safety limits. Generally, only the safety limit and associated limiting conditions for operation (LCOs) and surveillance requirements (SRs) are included in the plant's TSs. The safety limit associated with CBT is typically focused on an accurate quantification of the uncertainty of the CBT model and may also include the quantification of additional uncertainties as well.

The third regulation associated with a CBT is in 10 CFR 50.34, which focuses on defining the information that a licensee must present to ensure safe operation. Specifically, 10 CFR 50.34(a)(4) requires that the Preliminary Safety Analysis Report (PSAR) include determination of the margins of safety during normal operation and AOOs. One of these is the margin to CBT, which verifies that fuel failure is precluded during normal operation and AOOs through analysis.

The fourth regulation associated with a CBT appears in 10 CFR Part 50, Appendix B. It requires licensees to include certain structures, systems, and components (SSCs) in a quality assurance (QA) program that satisfies specific criteria. Appendix B, Criterion III, requires that specified design control measure be applied to the design of safety-related SSCs, and these measures apply to safety analyses for these SSCs. The CBT model is a key component of the safety analysis subject to 10 CFR Part 50, Appendix B.

The NRC has not created or endorsed guidance specifically on the review of CBT models. Therefore, based on several previous reviews, the NRC staff have generated detailed criteria which CBT models should meet, and have provided those criteria as the basis for this review.

3.0 TECHNICAL EVALUATION

The submittal describes how the model was developed from experimental data, the model's behavior, and how the model will be applied. The NRC staff's technical evaluation is focused on determining if the critical boiling model is acceptable for use in reactor safety license calculations (i.e., that the model can be trusted). To perform this evaluation, the NRC staff used a framework similar to the framework used in the NRC staff's safety evaluation (SE) of the

ORFEO-CHF correlation (Ref. 22), the ACE/ATRIUM-11 CPR correlation (Ref. 23), and the NuScale Power CHF correlation (Ref. 24).

3.1 Review Framework for Critical Boiling Transition Models

This section discusses the review framework for CBT models used in this review. This framework is expressed using concepts from Goal Structuring Notation (GSN). In GSN, the safety case is presented as a structure which contains multiple goals. The top goal, is a high-level statement we wish to demonstrate as true. It would be very difficult to demonstrate this statement is true with some set of basic evidence. Therefore, the top goal is decomposed into a set of goals (i.e., sub-goals). In this decomposition, proving each sub-goal is true is considered equivalent to proving the top goal is true. Further, each sub-goal is further decomposed, and so on, until a set of goals are obtained which can be demonstrated to be true through some basic evidence. For clarity, this last set of goals which is demonstrated to be true via evidence are termed *base goals*.

For CBT models, the top goal is: *The CBT is acceptable for use in reactor safety analyses.* Based on the author's experience reviewing these models, a study of previous SEs, and multiple discussions with various industry experts, this goal is decomposed into the three sub-goals given in
Figure 1.

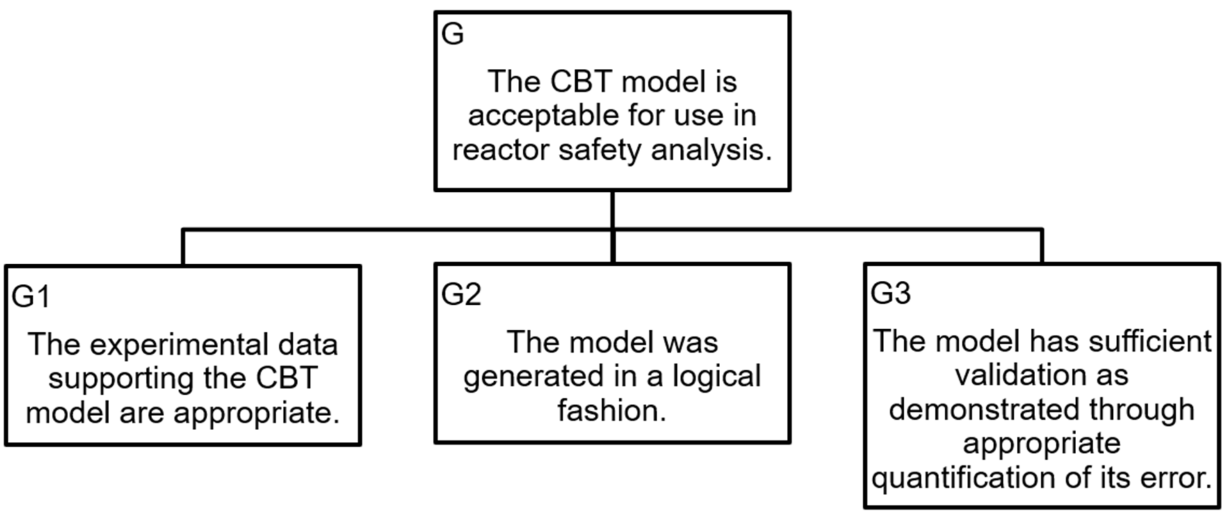

Figure 1: Decomposing G - Main Goal

3.1.1 Experimental Data

Experimental data is the cornerstone of a CBT model. Not only is the data used to generate the coefficients of the model and validate the model, but previous data is often used to generate the model's form. Therefore, it is essential that the experimental data is appropriate.

Demonstrating the experimental data is appropriate is accomplished using the three sub-goals given in
Figure **2** below.

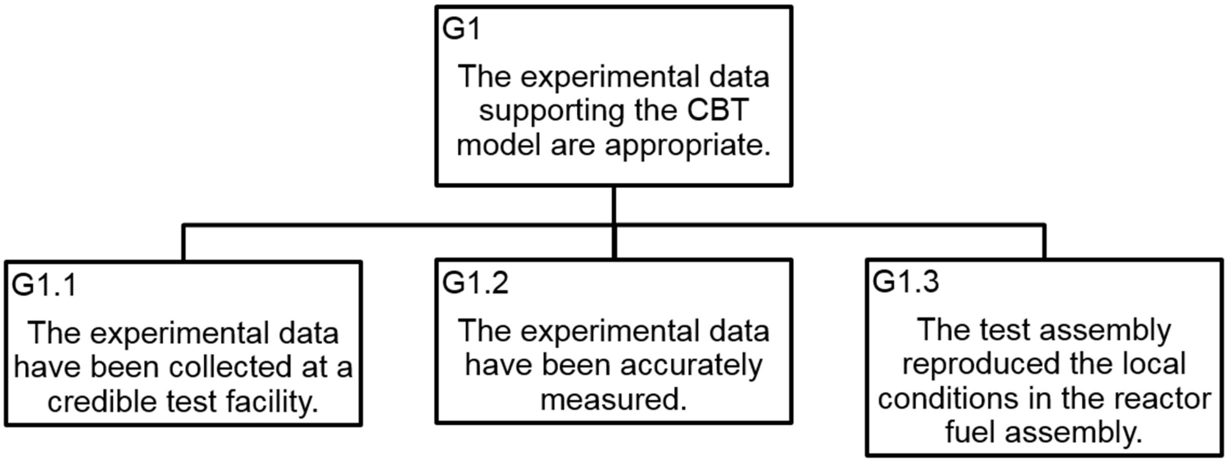

Figure 2: Decomposing G1 - Experimental Data

3.1.1.1 Credible Test Facility

The first sub-goal in demonstrating that the experimental data are appropriate is to demonstrate that the test facility is credible. This is typically demonstrated using the two sub-goals as given in
Figure 3 below.

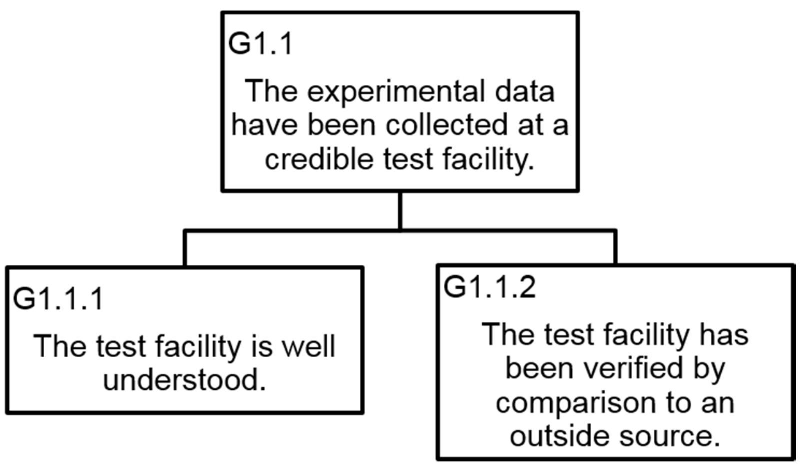

Figure 3: Decomposing G1.1 - Credible Test Facility

No further decompositions of the sub-goals were deemed useful. Therefore, the evidence demonstrating the following goals were met are provided below.

3.1.1.1.1 Test Facility Description

Test Facility Description

The test facility is well understood.

G1.1.1, Review Framework for Critical Boiling Transition Models

In the initial submittal, Westinghouse provided a description of the test facility, including the various loop components as well as a description of the heater rods and the instrumentation. The test facility setup is consistent with the setup of other experimental facilities used to conduct similar experiments. The specific type of heater rods used in the FRIGG loop are commonly used to perform CBT testing. The test facility has been appropriately instrumented to measure the pressure (both absolute and differential), inlet subcooling, bundle power, and inlet mass flux.

In response to RAI-SNPB-01, Westinghouse provided references for the measurement system, the test procedure, and quality assessments performed after each of the testing campaigns. Westinghouse also confirmed that the QA program is in compliance with Appendix B to 10 CFR Part 50 and has been previously audited by the NRC staff. Additionally, the NRC staff were able to visit the test facility to better understand it.

The description of the facility provided by Westinghouse, along with the NRC staff's visit, provided the NRC staff with a clear understanding of the test facility, what data were obtained, and how the data were obtained. Because Westinghouse has described the test facility and provided references for the facility, the NRC staff has determined that this goal has been met.

3.1.1.1.2 Test Facility Comparison

Test Facility Comparison

The test facility has been verified by comparison to an outside source.

G1.1.2, Review Framework for Critical Boiling Transition Models

In the initial submittal, Westinghouse did not provide any discussion of the comparison of the FRIGG loop to an outside source. In response to RAI-SNPB-02, Westinghouse provided details of a comparison between FRIGG and ATLAS data. The comparison demonstrated that both facilities had very similar predictions of CP for the same test bundle.

Because the FRIGG loop was compared to the ATLAS facility and demonstrated to have very similar predictions, the NRC staff has determined that this goal has been met.

3.1.1.2 Accurate Data

The second sub-goal in demonstrating that the experimental data are appropriate is to demonstrate that the experimental data has been accurately measured. This is typically demonstrated using the seven sub-goals as given in Figure **4** below.

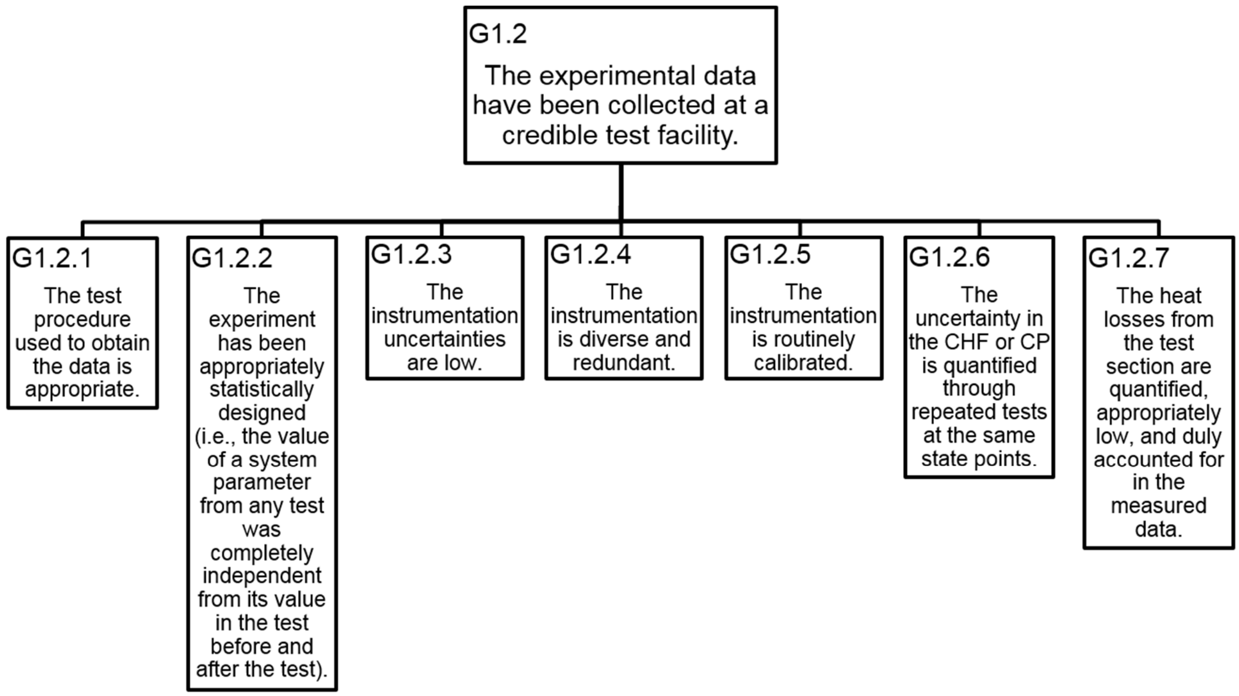

Figure 4: Decomposing G1.2 - Accurate Data

No further decompositions of the sub-goals were deemed useful. Therefore, the evidence demonstrating the following goals were met are provided below.

3.1.1.2.1 Test Procedures

Test Procedures
The test procedure used to obtain the data is appropriate.
G1.2.1, Review Framework for Critical Boiling Transition Models

In the initial submittal Westinghouse provided a basic description of its test procedure. In response to RAI-SNPB-10, Westinghouse described how each state point was reached, including the approach to dryout, the steady state criteria, and the dryout criteria. Further, in response to RAI-SNPB-01 and RAI-SNPB-11, Westinghouse provided a reference to the test procedures.

Because Westinghouse is applying a logical approach to dryout by narrowing in on a state point, ensuring that a steady state has been reached, ensuring that any deviations during the approach to dryout are small, and ensuring there is a consistent definition applied in identifying dryout, the NRC staff has determined that this goal has been met.

3.1.1.2.2 Statistical Design of Experiment

Statistical Design of Experiment

The experiment has been appropriately statistically designed (i.e., the value of a system parameter from any test was completely independent from its value in the test before and after it.)

G1.2.2, Review Framework for Critical Boiling Transition Models

In response to RAI-SNPB-12, Westinghouse described its method for determining the state points. Westinghouse stated that a parameter variation matrix was formed and a randomization procedure was applied. Westinghouse also provided details on the order of choosing parameters. **[**

]^{a,c}

Because Westinghouse is selecting random state points inasmuch as the testing allows and used repeated test points to ensure there was no bias during testing, the NRC staff has determined this goal has been met.

3.1.1.2.3 Instrumentation Uncertainties

Instrumentation Uncertainties

The instrumentation uncertainties are low.

G1.2.3, Review Framework for Critical Boiling Transition Models

In the initial submittal, Westinghouse provided a list of the instrumentation uncertainties. In response to RAI-SNPB-13, Westinghouse clarified the uncertainty of its mass flux measurement.

Because these instrumentation uncertainties are relatively small **[**
]^{a,c} and within the range of normal instrumentation, the NRC staff has determined this goal has been met.

3.1.1.2.4 Diverse Instrumentation

Diverse Instrumentation
There is diverse and redundant instrumentation.
G1.2.4, Review Framework for Critical Boiling Transition Models

In response to RAI-SNPB-14, Westinghouse described the instrumentation of the test.
[

]a,c

Because Westinghouse is **[**

]a,c the NRC staff has determined this goal has been met.

3.1.1.2.5 Instrumentation Calibration

Instrumentation Calibration
The instrumentation is routinely calibrated.
G1.2.5, Review Framework for Critical Boiling Transition Models

In response to RAI-SNPB-15, Westinghouse confirmed that instrumentation is routinely calibrated **[** **]**a,c

Because Westinghouse's procedures require instrumentation calibration on a reasonable basis, the NRC staff has determined that this goal has been met.

3.1.1.2.6 Repeated Test Points

Repeated Test Points
The uncertainty in the critical heat flux or critical power is quantified through repeated tests at the same state points.
G1.2.6, Review Framework for Critical Boiling Transition Models

In the initial submittal, Westinghouse provided an estimate of the uncertainty in the CP of **[ ]**[a,c] but did not provide details on how it obtained that estimate. In response to RAI-SNPB-16, Westinghouse stated the uncertainty in CP was determined based on assuming the **[**

][a,c] While this provides an estimate of the sensitivity of the CPR model to input uncertainties, the NRC does not believe it provides an estimate of the uncertainty of the CPR itself.

In response to RAI-SNPB-17, Westinghouse determined the variation in the D5 CPR prediction between similar tests. However, that variation does not separate out the repeatability (i.e., uncertainty) of the experimental facility. Instead, it convolutes that repeatability with other uncertainties in the D5 model. In the supplemental response to RAI-SNPB-17, Westinghouse provided additional information on this repeatability measure, including a comparison between the predicted CPR and the measured CPs for multiple repeat test points. That comparison confirmed that the difference in measured CP is approximately equal to the difference in the CPR for each of the repeated test points. Because the difference in measured CPs were very small for repeated test points, even less ~~then~~ than the estimated uncertainty in the TR, the NRC staff has determined that this goal has been met.

3.1.1.2.7 Quantified Heat Losses

Quantified Heat Losses
The heat losses from the test section is quantified, appropriately low, and duly accounted for in the measured data.
G1.2.7, Review Framework for Critical Boiling Transition Models

In response to RAI-SNPB-18, Westinghouse confirmed that the heat balance is performed at the start of a test campaign and confirmed that the heat losses were appropriately low. During the audit (Ref. 14), Westinghouse provided additional details on the heat loss testing and confirmed that the heat losses are applied directly to the CP, reducing it in a conservative manner.

Because Westinghouse is confirming the heat losses before each test campaign and using those heat losses to conservatively reduce CP, the NRC staff has determined that this goal has been met.

3.1.1.3 Reproduced Local Conditions

The third sub-goal in demonstrating that the experimental data are appropriate is to demonstrate that the local conditions in the reactor have been reproduced in the experiment.

This is typically demonstrated using the five sub-goals as given in Figure **5** below.

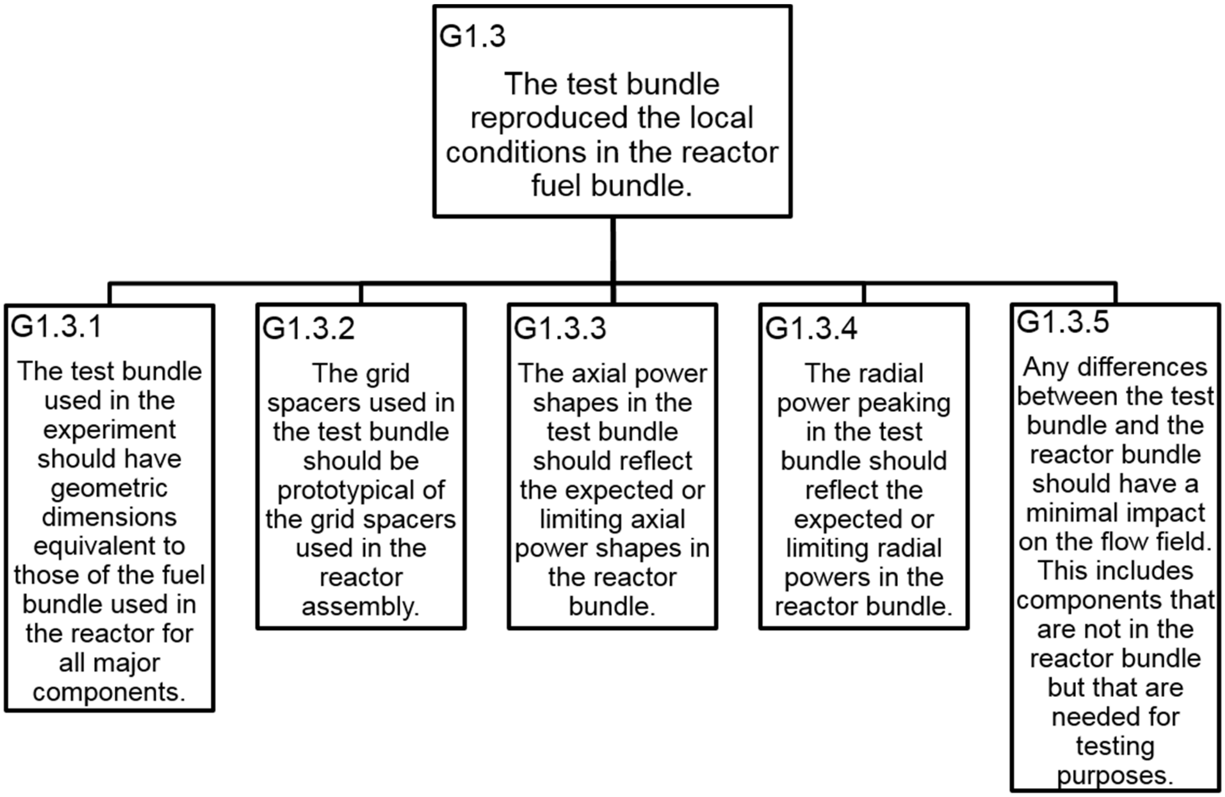

Figure 5: Decomposing G1.3 – Reproduced Local Conditions

No further decompositions of the sub-goals were deemed useful. Therefore, the evidence demonstrating the following goals were met are provided below.

3.1.1.3.1 Equivalent Geometries

Equivalent Geometries
The test bundle used in the experiment should have equivalent geometric dimensions to that of the fuel bundle used in the reactor for all major components.
G1.3.1, Review Framework for Critical Boiling Transition Models

In the initial submittal, Westinghouse provided a description of the test bundle. The bundle is a prototypical SVEA 5x5 sub-bundle with 24 heater rods. It contains three part-length rods, of which two are two-thirds length and one is one-third length. To ensure the inlet flow distribution in the testing is similar to that in the reactor, an orifice plate is installed at the inlet of the flow channel. The pressure drop of this orifice plate is similar to the debris filter used in SVEA-96 Optima3 fuel. The rod diameter of the test bundle is consistent with the rod diameter of the fuel bundle.

While most of the test bundle dimensions were very similar to the fuel bundle, some dimensions of the test bundle were slightly different than those from the fuel bundle. Because these dimensions may impact dryout, additional information was requested in RAI-SNPB-04. In the response, Westinghouse **[**

][a,c]

Westinghouse also discussed the differences in flow areas between the test channel and the fuel bundle. The flow area of the test channel is slightly smaller than that of the fuel bundle **[** **]**[a,c] This mostly due in the corners where the water cross walls are welded to the outer channel section. Westinghouse confirmed that the inner dimensions of the channel and the rod pitch were not impacted. The NRC staff agrees that this small difference would have a minimal impact on the CP performance.

Further, after the testing, Westinghouse identified an axial shift in a number of grid spacers. In the original submittal, Westinghouse provided a brief analysis of this spacer grid shift but did not fully address the issue. Therefore, the NRC staff requested additional information in RAI-SNPB-06. In the response, Westinghouse provided a more detailed description of the spacer shift. **[**

][a,c]

[

][a,c]

[

]a,c

In the initial submittal, Westinghouse provided details on the part-length rods. Westinghouse stated that [

]a,c However, Westinghouse did not discuss the impact of these differences; therefore, additional information was requested in RAI-SNPB-09. In response to this RAI, Westinghouse [

]a,c

Finally, while the SVEA-96 Optima3 bundle has four sub-bundles, only one of the sub-bundles is used in the tested assembly. This was previously reviewed by the NRC in the D4 CPR correlation (Ref. 5) and is not addressed here.

While there were slight differences between the test bundle and the fuel bundle, those differences were either accounted for in the application of the D5 model or were ~~or were~~ determined to have a minimal impact on the model's prediction as explained above, therefore the NRC staff has that this goal has been met.

3.1.1.3.2 Equivalent Grid Spacers

Equivalent Grid Spacers

The grid spacers used in the test bundle should be prototypical of the grid spacers used in the reactor assembly.

G1.3.2, Review Framework for Critical Boiling Transition Models

In the initial submittal, Westinghouse discussed the spacer grid designs used in the Optima3 assembly. In response to RAI-SNPB-05, Westinghouse confirmed that there was no difference between the spacer grid types used in the test bundle and those used in the reactor fuel bundle.

Because there is no difference between the grid types used in the test and fuel bundle, the NRC staff has determined that this goal has been met.

3.1.1.3.3 Axial Power Shapes

Axial Power Shapes

The axial power shapes in the test bundle should reflect the expected or limiting axial power shapes in the reactor bundle.

G1.3.3, Review Framework for Critical Boiling Transition Models

In the initial submittal, Westinghouse provided details on the local powers used in the CP testing and stated that the local power influences were fully captured. There are a very large number of combinations of local powers possible, not all of which could realistically be tested. Westinghouse did not provide an explanation of its methodology for choosing the axial powers tested and why those powers were sufficient to cover the complete range of possible axial powers in the reactor fuel bundle. Therefore, the NRC staff requested additional information in RAI-SNPB-08. In the response, Westinghouse discussed the justification for using the bottom- and top-peaked power shapes to bound those power shapes typically experienced in BWR fuel. **[**

][a,c]

Because the power shapes tested represent those experienced at the beginning of life (bottom-peaked), end of life (top-peaked), and under the typically most severe event (top-peaked), and because the shapes tested are consistent with the power shapes commonly tested for CP models, the NRC staff has determined that this goal has been met.

3.1.1.3.4 Radial Power Shapes

Radial Power Shapes

The radial power peaking in the test bundle should reflect the expected or limiting radial powers in the reactor bundle.

G1.3.4, Review Framework for Critical Boiling Transition Models

For BWR CPR analysis, the radial power dependence is captured in the R- or K- factors. These factors are used in a single-channel model to account for all radial power dependences, and when combined with the additive constants account for all radial dependences in the fuel bundle. Therefore, the NRC staff expects the radial power shapes that are tested to be sufficient to: (1) obtain additive constants and (2) ensure that a complete set of R-factors or K- factors can be calculated.

In the initial response to RAI-SNPB-07, Westinghouse provided the justification for the radial powers tested. The testing focused on **[**

][a,c]

Because Westinghouse's testing focused on ensuring that the radial power distributions applied in the experiment covered the range needed to obtain key values for the CPR model for each rod and were also consistent with actual bundle design, the NRC staff has determined that this goal has been met.

3.1.1.3.5 Differences between Test and Reactor

Differences between Test and Reactor

Any differences between the test bundle and the reactor bundle should be addressed. This includes components which are not in the reactor bundle but are needed for testing purposes.

G1.3.5, Review Framework for Critical Boiling Transition Models

Except for those differences addressed above, there were no differences between the prototypical test assembly and the assembly which will go into reactors. However, during the review of this TR, the NRC staff became aware of operating experience which raised the question of differences between the phenomena observed during testing and the phenomena present in reactors. The operating experience was a failed fuel rod at the Leibstadt Nuclear Power Plant (NPP) in Switzerland that led to the discovery of v-shaped marks on fuel rods in 47 SVEA-96 Optima2 fuel bundles from five recent operating cycles. The v-shaped marks, initially believed to be fuel rod cladding oxidation, were later determined to be mostly a zinc-rich crud.

While the single fuel rod failure and v-shaped marks were associated with SVEA-96 Optima2, neither Westinghouse nor the NRC staff believed the slight differences between Optima2 and Optima3 assemblies designs would have had a major impact on the underlying phenomena. Additionally, while the CPR model used for Optima2 fuel is the D4 model, and D5 is under review here, both models predicted substantially similar CPs for bundles in Leibstadt NPP. For these two reasons, the NRC staff considered it necessary to address this issue for the SVEA-96 Optima3 fuel design and the associated D5 CP model. The same arguments used to address this issue could be made for SVEA-96 Optima2 and the D4 model. Due to the length of the discussion concerning this issue, it will be discussed in further detail in Section 3.2, "Single fuel rod failure and multiple v-shaped marks at Leibstadt NPP."

3.1.2 Model Generation

There are numerous ways to generate the CBT model. While some methods of generation are based on physics, the model is still largely empirical in nature. Therefore, there is no single correct way to generate the model. The form of the model is often based on previous model forms, machine learning techniques, and engineering judgment. Demonstrating the model generation is appropriate is accomplished using the two sub-goals given in Figure **6** below.

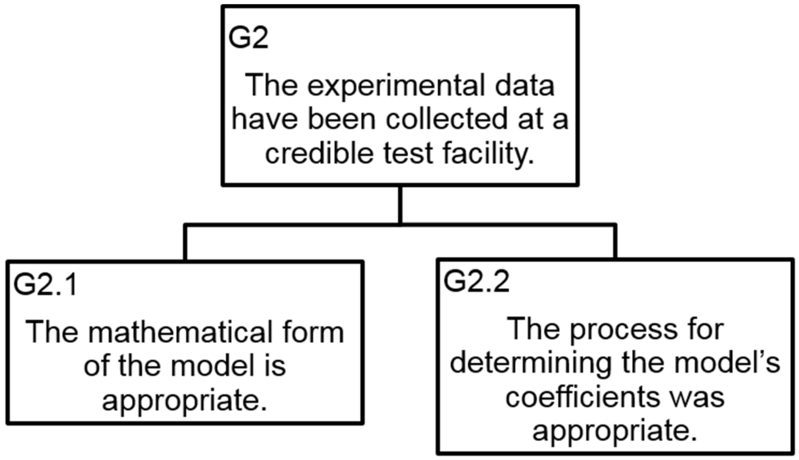

Figure 6: Decomposing G2 – Model Generation

3.1.2.1 Appropriate Mathematical Model

The first sub-goal in demonstrating that the model was generated in a logical fashion is to demonstrate that the model's form is appropriate. This is typically demonstrated using the two sub-goals as given in Figure **7** below.

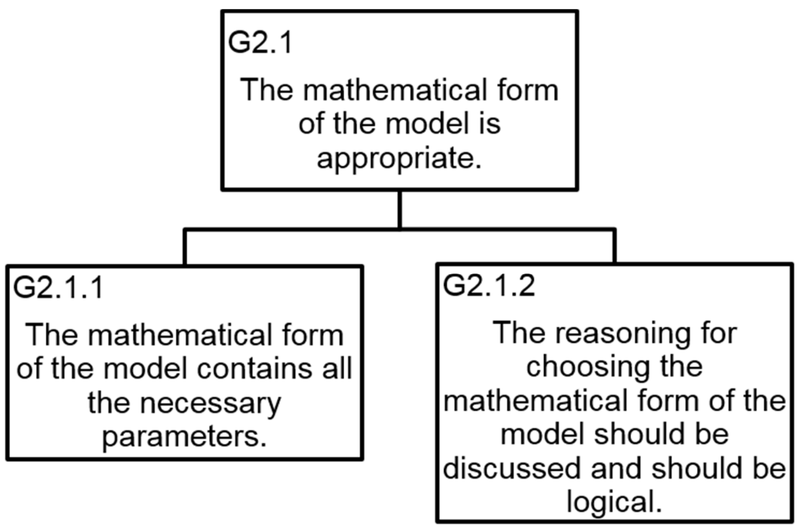

Figure 7: Decomposing G2.1 – Model Form

No further decompositions of the sub-goals were deemed useful. Therefore, the evidence demonstrating the following goals were met are provided below.

3.1.2.1.1 Model Parameters

Model Parameters

The mathematical form of the model contains all necessary parameters.

G2.1.1, Review Framework for Critical Boiling Transition Models

Westinghouse stated that the D5 model form was derived using trends observed in the testing database. Because the model form contains those key parameters typically found to be important in modeling dryout, the NRC staff has determined that this goal has been met.

3.1.2.1.2 Model Form

Model Form

The reasoning for choosing the mathematical form of the model should be discussed and be logical.

G2.1.2, Review Framework for Critical Boiling Transition Models

In the initial submittal, Westinghouse discussed the mathematical form chosen for the steady state D5 model as well as the sub-models supporting it. The steady state form of the model and its supporting models were discussed in sufficient detail to provide understanding to the NRC staff. The transient form of the model was briefly discussed, but adequate detail was not provided for the NRC staff to understand how the transient form of the model was derived. Therefore, additional information was requested in RAI-SNPB-19. In the response, Westinghouse discussed each parameter in the D5 model, defined the parameter, defined where the parameter was evaluated, and at what time it was evaluated in the simulation. These tables greatly increased the NRC staff's understanding of the mathematical model form of the D5 model.

Westinghouse used a Lagrangian transformation on the model for transient dryout. The NRC considered this transformation appropriate, as the flow field in the fuel assembly at any specific time is continually changing and can only impact the flow field above it (and likewise be impacted by the flow field below it) at the speed of the flow itself. Ultimately, the demonstration that this method is acceptable was provided in its use in predicting the CP during the transients testing. The transient tests demonstrated that the transient version of the D5 CPR model, and therefore its use of the Lagrangian transformation, was able to conservatively or accurately predict the transient dryout performance, as discussed below in Section 3.1.3.5.3, "Transient Prediction."

Further, Westinghouse's mathematical model for D5 **[**

][a,c] Therefore, additional information was requested in RAI-SNPB-20. In the

response, Westinghouse [

]a,c

[

]a,c"

Because Westinghouse has provided details defining the functions and variables which comprise the D5 model, therefore NRC staff has determined that this goal has been met.

3.1.2.2 Model Coefficient Generation

The second sub-goal in demonstrating that the model was generated in a logical fashion is to ensure that the process for generating the model's coefficients is appropriate. This is typically demonstrated using the three sub-goals as given in
Figure **8** below.

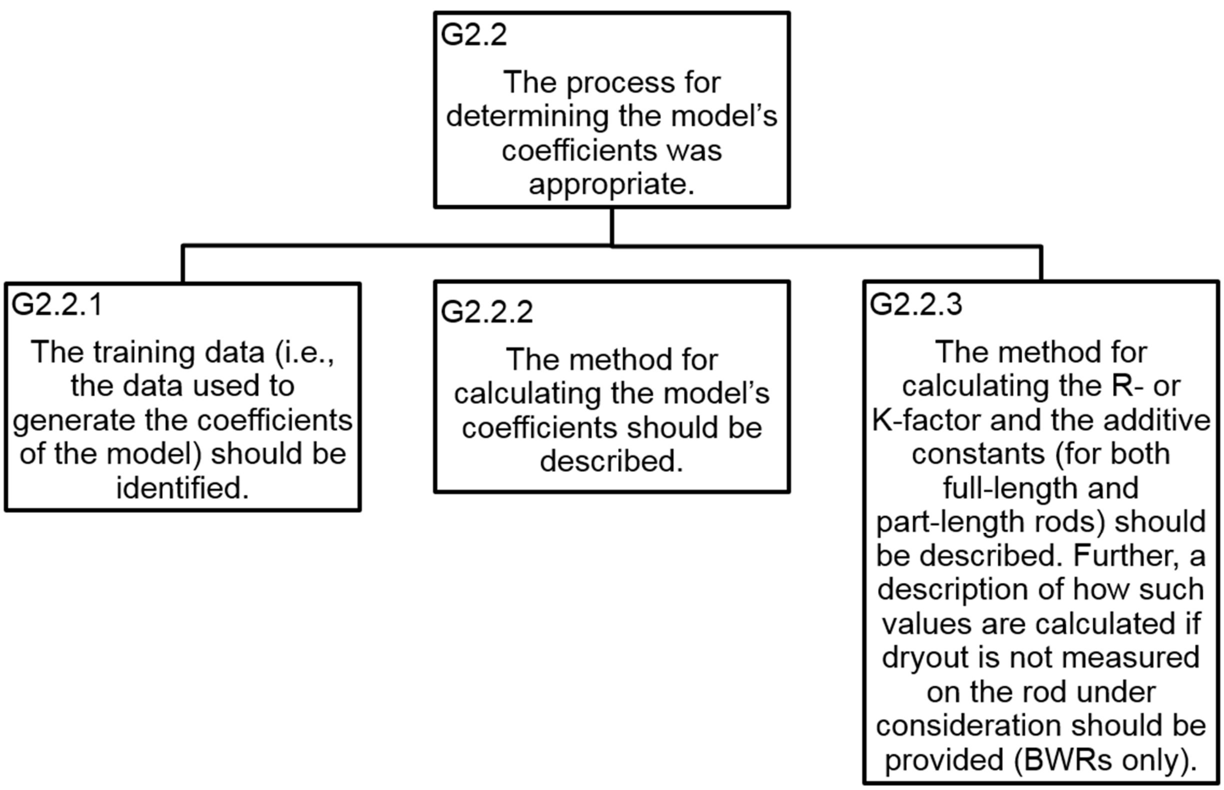

Figure 8: Decomposing G2.2– Model Coefficient Generation

No further decompositions of the sub-goals were deemed useful. Therefore, the evidence demonstrating the following goals were met are provided below.

3.1.2.2.1 Training Data

Training Data
The training data (i.e., the data used to generate the coefficients of the model) should be identified.
G2.2.1, Review Framework for Critical Boiling Transition Models

In the initial submittal, Westinghouse identified that **[** **]**^{a,c} of the data was used to train the D5 model. Therefore, the NRC staff has determined that this goal has been met.

3.1.2.2.2 Coefficient Generation

Coefficient Generation
The method for calculating the model's coefficients should be described.
G2.2.2, Review Framework for Critical Boiling Transition Models

Westinghouse provided a summary of the method used to develop the coefficients. In the response to RAI-SNPB-21, Westinghouse provided additional details to fully describe the method for calculating the model's coefficients. **[**

]^{a,c}

In the initial submittal, Westinghouse described analysis performed with MEFISTO which **[**

]^{a,c} In the response to RAI-SNPB-22, Westinghouse added that additional testing had been performed since the publication of the TR and dryout data was obtained for the 1/3 part-length rod. This data confirmed that the rod constant used for the 1/3 part-length rod in the D5 model was conservative.

Because Westinghouse's method for generating the model's coefficients was fully described and reasonable, the NRC staff has determined that this goal has been met.

3.1.2.2.3 BWR Specific Parameters

> **BWR Specific Parameters**
>
> *The method for calculating the R or K factors and the additive constants (for both full length and part length rods) should be described. Further, a description should be provided of how such these values are calculated if dryout is not measured on the rod under consideration.* **(BWRs only)**.
>
> G2.2.3, Review Framework for Critical Boiling Transition Models

In the initial submittal, Westinghouse provided the equations used to generate the R-factors and rod constants. In the response to RAI-SNPB-21, Westinghouse described the process for obtaining the R factors and the additive constants. Westinghouse described **[**

][a,c]

Because Westinghouse's method for generating the BWR specific parameters was fully described, the NRC staff has determined that this goal has been met.

3.1.3 Model Validation

Validation is the accumulation of evidence which is used to assess the claim that a model can predict a real physical quantity (Ref. 26). Thus, validation is a never-ending process as more evidence can always be obtained to bolster this claim. However, at some point, when the accumulation of evidence is considered sufficient to make the judgment that the model can be trusted for its given purpose, the model is said to be validated. Demonstrating that the model validation is appropriate is accomplished using the five sub-goals given in Figure **9** below.

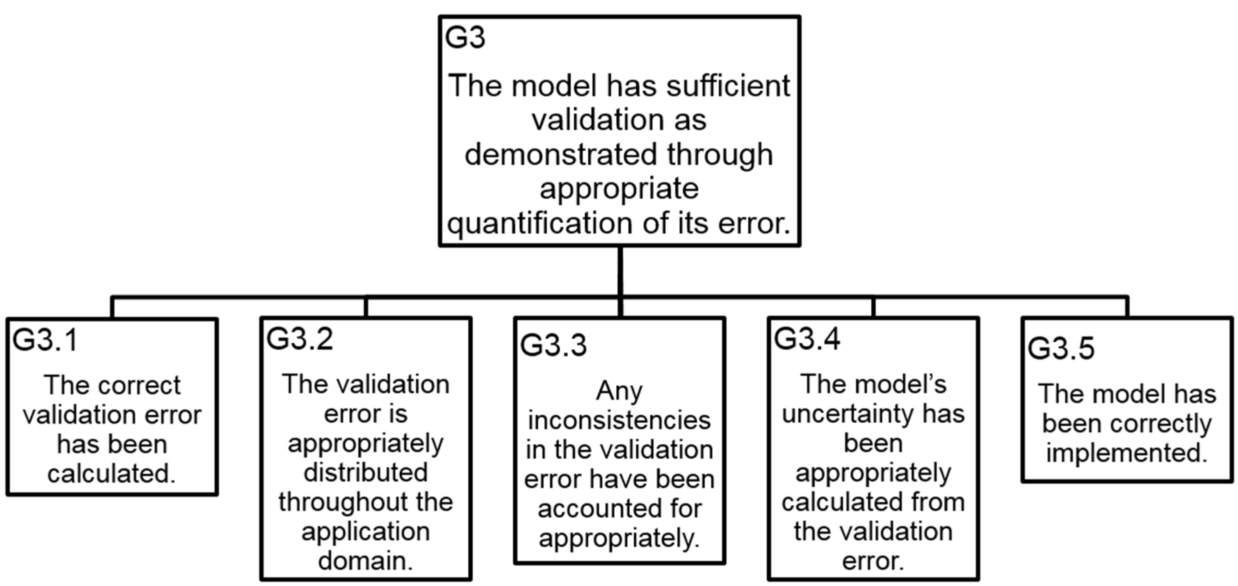

Figure 9: Decomposing G3 – Model Validation

3.1.3.1 Validation Error

Validation Error
The correct validation error has been calculated.
G3.1, Review Framework for Critical Boiling Transition Models

For CP correlation, the validation error should be based on the CP from the experimental tests and the predicated CP of the test assembly. Because Westinghouse is using these terms to calculate the error in CPR (i.e., the validation error), and has provided this data to the NRC in Reference 9, the NRC staff has determined that this goal has been met.

3.1.3.2 Data Distribution

The first sub-goal in demonstrating that the model's validation was appropriate is to demonstrate that the data is appropriately distributed throughout the application domain. This is typically demonstrated using the six sub-goals as given in
Figure **10** below.

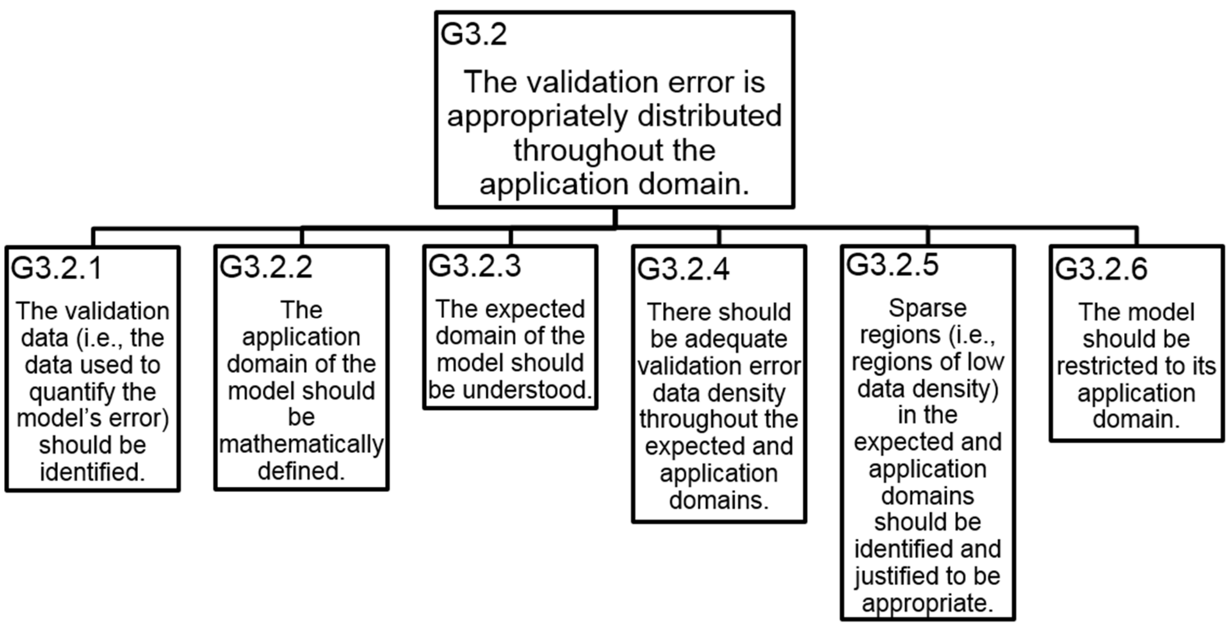

Figure 10: Decomposing G3.2 – Data Distribution

No further decompositions of the sub-goals were deemed useful. Therefore, the evidence demonstrating the following goals were met are provided below.

3.1.3.2.1 Validation Data

Validation Data
The validation data (i.e., the data used to quantify the model's error) should be identified.
G3.2.1, Review Framework for Critical Boiling Transition Models

In the initial submittal, Westinghouse identified that **[** **]**^{a,c} Therefore, the NRC staff has determined that this goal has been met.

3.1.3.2.2 Application Domain

Application Domain
The application domain of the model should be mathematically defined.
G3.2.2, Review Framework for Critical Boiling Transition Models

In the submittal, Westinghouse provided the boundaries of the application domain of the D5 correlation in a table in the Section 5, "Conclusion." That application domain is given in table 6-7 of the TR. The NRC staff found this domain reasonable as it was similar to other such domains.

Because Westinghouse provided this information, the NRC staff has determined that this goal has been met.

3.1.3.2.3 Expected Domain

Expected Domain
The expected domain of the model should be understood.
G3.2.3, Review Framework for Critical Boiling Transition Models

In the initial submittal and subsequent response to RAI-SNPB-03, Westinghouse provided the following plots showing the data collected and the range of typical application. This range of typical application is defined as the *expected domain*:

- Pressure vs. Mass Flux (Figure 4-5)
- Pressure vs. Subcooling (Figure 4-6)
- Pressure vs. R-factor (RAI-SNPB-03, Figure 1)
- Subcooling vs. Mass Flux (Figure 4-7)
- R-factor vs. Mass Flux (Figure 4-8)
- Subcooling vs. R-factor (RAI-SNPB-03, Figure 2)

From these plots, the expected domain can be understood. Because Westinghouse has provided the plots which identify the expected domain, the NRC staff has determined that this goal has been met.

3.1.3.2.4 Data Density

Data Density
There should be adequate data density throughout the expected and application domains.
G3.2.4, Review Framework for Critical Boiling Transition Models

In the initial submittal and subsequent response to RAI-SNPB-03, Westinghouse provided the figures which define the application and expected domain, as discussed above. Westinghouse provided further supplemental information in References 14 and 18. A review of the data density in this domain is limited to 2D comparisons of each of the most important parameters (pressure, mass flux, subcooling, and R-factor).

<u>Pressure vs Mass Flux</u>

[

][a,c]

<u>Pressure vs Subcooling</u>

[

][a,c]

<u>Pressure vs R-Factor</u>

[

][a,c]

<u>Subcooling vs. Mass Flux</u>

[

]a,c

<u>R-factor vs. Mass Flux</u>

[

]a,c

<u>Subcooling vs. R-factor</u>

[

] a,c

With the exception of the sparse region identified which will be addressed below in Section 3.1.3.2.5, "Sparse Regions," because Westinghouse has provided details of the data density in the expected and application domains and that density is consistent with the data density commonly expected in CP testing, the NRC staff has determined this goal has been met.

3.1.3.2.5 Sparse Regions

Sparse Regions
Sparse regions (i.e., regions of low data density) in the expected and application domains should be identified and justified to be appropriate.
G3.2.5, Review Framework for Critical Boiling Transition Models

The NRC staff identified the following sparse regions inside the expected and application domains in Section 3.1.3.2.4, Data Density, above:

(A) A region defined by a [ ]a,c
(B) A region defined by a [ ]a,c
(C) A region defined by [ ]a,c
(D) A region defined by [ ]a,c
(E) A region defined by [ ]a,c
(F) A region defined by [ ]a,c
(G) A region defined by [ ]a,c
(H) A region defined by [ ]a,c

To address the use of the D5 model in sparse region (A), Westinghouse stated in response to RAI-SNPB-25 and RAI-SNPB-26 that while the correlation will be applied in regions [

]a,c Westinghouse has provided data which demonstrates that the critical quality increases as the mass flux decreases. Therefore, by using a [

]a,c The NRC staff finds that this is a conservative implementation of the D5 model and therefore adequate justification the sparse region (A) in the application domain.

To address the use of the D5 model in sparse region (B), Westinghouse stated in response to RAI-SNPB-27 the correlation will be applied in regions [

]a,c Westinghouse further stated that the high mass flux and lower pressure region in the application domain is of limited importance in practical application, which is also reiterated by this region being outside the expected domain. The NRC staff finds that such a sparse region is common in testing data, and that the data obtained near the sparse region and the prediction of that data demonstrates that there is adequate justification for the sparse region (B) in the application domain.

To address the use of the D5 model in sparse region (C), in response to RAI-SNPB-28 Westinghouse stated that the model's behavior with subcooling has a linear trend, and that linear trend has been observed in previous fuel designs, therefore intermediate data is not required. The NRC agrees that this trend and the use of historical evidence justifies sparse region (C) in the application domain.

To address the use of the D5 model in sparse regions (D), in response to RAI-SNPB-28 Westinghouse stressed that high R-factor are generally not limiting, as having multiple rods closer to dryout is more limiting (i.e., results in a lower CP) than having a single rod closer to dryout. Additionally, the use of the D5 model at these high R-factors is outside of its expected range of use. The NRC agrees that the facts that this region is likely to not be a limiting region and is not in the expected domain justifies sparse region (D) in the application domain.

To address the use of the D5 model in sparse region (E) – (G), in response to RAI-SNPB-28 Westinghouse stated that these R-factor values are characterized by off-nominal conditions in mass flux, pressure, or inlet subcooling. That is, [

]a,c

The most limiting case is with the lowest R-factors (as this means more rods are closer to dryout, rather than a single rod being closer to dryout), and this range of low R-factors was well tested. The NRC agrees that these intermediate R-factors would likely not result in limiting conditions and justifies the sparse regions (E) – (G) in the application domain.

To address the use of the D5 model in sparse region (H), in the supplemental response to RAI-SNPB-03, Westinghouse decided to monitor the reload design process and ensure that sub-bundles with [

]a,c The NRC agrees that this monitoring justifies the sparse region (H) in the application domain.

Because Westinghouse satisfactorily justified each of the sparse regions in the application domain, the NRC staff has determined that this goal has been met.

3.1.3.2.6 Restricted Domain

Restricted Domain
The model should be restricted to its application domain.
G3.2.6, Review Framework for Critical Boiling Transition Models

In the response to RAI-SNPB-24, Westinghouse confirmed that should the D5 model be used outside of its application domain, the computer code would issue a warning. This would prompt an investigation to ensure that the sub-bundle has no realistic possibility of influencing the results of the calculation (i.e., ensure the sub-bundle in question is far from being CPR limiting for the entire core).

Because Westinghouse is monitoring and enforcing the use of the D5 model, the NRC staff has determined that this goal has been met.

3.1.3.3 Inconsistencies in the Model's Error

The second sub-goal in demonstrating that the model's validation was appropriate is to demonstrate that the model error is consistent over the application domain. This is typically demonstrated using the three sub-goals as given in
Figure **11** below.

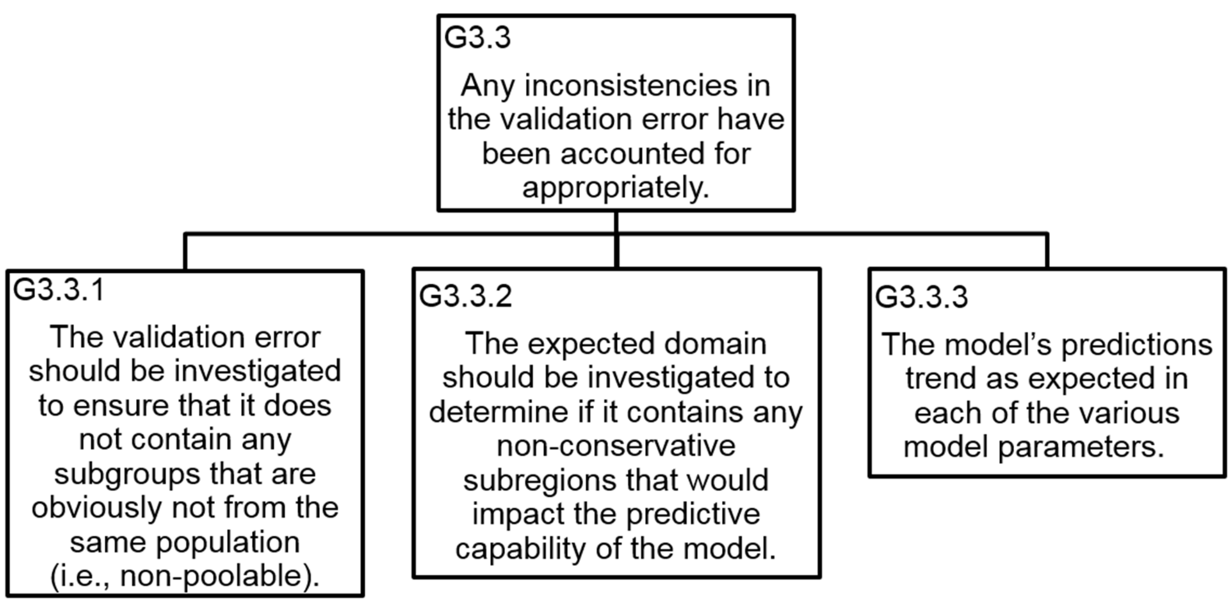

Figure 11: Decomposing G3.3 – Inconsistencies in the Model's Error

No further decompositions of the sub-goals were deemed useful. Therefore, the evidence demonstrating the following goals were met are provided below.

3.1.3.3.1 Poolability

Poolability
The validation error should be investigated to determine if it contains any sub-groups which are obviously not from the same population (i.e., not poolable).
G3.3.1, Review Framework for Critical Boiling Transition Models

In the initial submittal, Westinghouse provided statistical analysis of the predictions of the D5 model compared to test data. The NRC staff found that the data could be separated into one set of sub-groups based on axial power shapes. In response to RAI-SNPB-29, Westinghouse provided a statistical analysis of the CPR behavior for the three individual power shapes: bottom-peaked, cosine, and top-peaked. That analysis demonstrated that the CP behavior of the three sub-groups was similar and the proposed D5 model statistics are bounding for all three sub-groups. Because there was only one obvious set of sub-groups within the data and those three sub-groups were demonstrated to be poolable, the NRC staff has determined that this goal has been met.

3.1.3.3.2 Non-Conservative Subregions

Non-Conservative Subregions
The expected domain should be investigated to determine if it contains any non-conservative subregions that would impact the predictive capability of the model.
G3.3.2, Review Framework for Critical Boiling Transition Models

In the submittal, Westinghouse provided plots of the prediction error versus each model parameter in Chapter 6. None of these figures showed any signs of a non-conservative sub-region. Using a method similar to the one suggested by Kaizer (Ref. 25), the NRC staff analyzed the application domain for potential non-conservative subregions and found very little evidence of a non-conservative subregion. However, one potential region was identified which resulted in RAI-SNPB-37. The NRC staff believed they found a slight non-conservative subregion around **[ ]**[a,c] In the response, Westinghouse did confirm that there was slight non-conservative bias for this region. **[**

][a,c]

[

][a,c]

[

]a,c

[

]a,c

[

]a,c Therefore, the NRC staff felt it necessary to make the following condition: If it is likely that bundles with **[**

]a,c are either limiting or contributing to the SLMCPR bounding the cycle, those bundles shall have a bounding bias applied.

Additionally, the NRC staff requested clarification on Figures 4-9 and 4-10 in RAI-SNPB-31. Figures 4-9 and 4-10 **[**

]a,c

Because analysis of the application domain demonstrated that there was either no evidence of a non-conservative subregion in most of the application domain and that any potential sub-region would have negligible impact on the use of the D5 model, the NRC staff has determined that the expected domain does not contain any non-conservative subregions which would impact the predictive capability of the model. The NRC staff has concluded that this goal has been met.

3.1.3.3.3 Model Trends

Model Trends
The model's predictions trend as expected in each of the various model parameters.
G3.3.3, Review Framework for Critical Boiling Transition Models

In the initial submittal, Westinghouse provided numerous plots of model trends:

- Figures 4-9 through 4-28 demonstrate that the data used to train and validate the D5 model is trending correctly in terms of power, mass flux, pressure, and inlet subcooling.
- Figure 6-2 through Figure 6-5 demonstrated that the validation error was independent of each of D5's independent variables.
- Figures 6-8 and 6-9 demonstrate that the D5 model's prediction of CP is behaving as expected in terms of axial power shape and mass flux, and inlet subcooling and mass flux.
- Figure 6-10 through Figure 6-31 demonstrated that various subgroups of the validation error were independent of D5's independent variables.

Because these plots demonstrate the D5 model's predicted trends are consistent with previous experience and the D5 model's validation error is consistent over the range of each parameter, the NRC staff has determined that this goal has been met.

3.1.3.4 Quantified Model Error

The third sub-goal in demonstrating that the model's validation was appropriate is to demonstrate that the model error has been appropriately quantified over the application domain. This is typically demonstrated using the three sub-goals as given in
Figure **12** below.

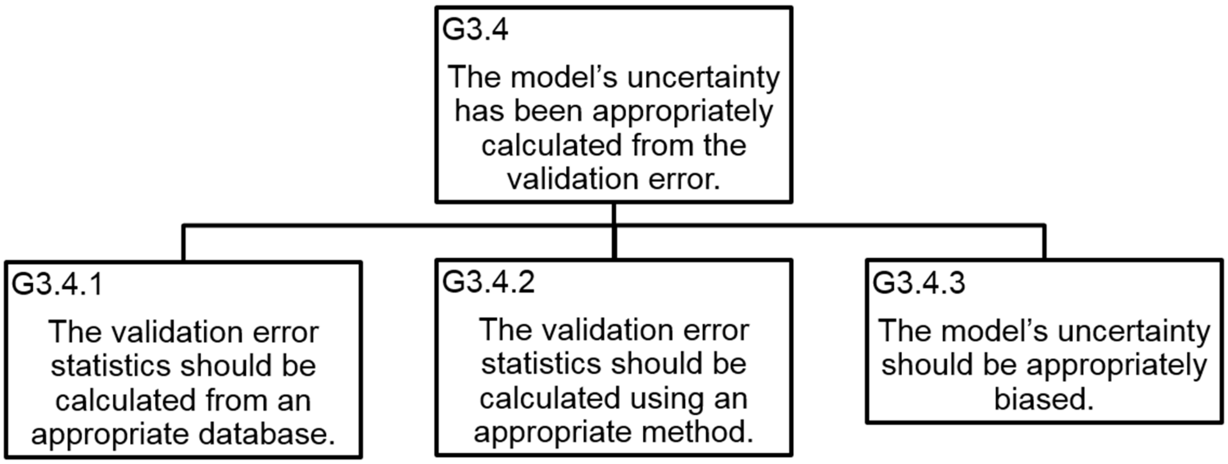

Figure 12: Decomposing G3.4 – Quantified Model Error

No further decompositions of the sub-goals were deemed useful. Therefore, the evidence demonstrating the following goals were met are provided below.

3.1.3.4.1 Error Database

Error Database

The validation error statistics should be calculated from an appropriate database.

G3.4.1, Review Framework for Critical Boiling Transition Models

In the initial submittal, Westinghouse identified that **[**

]^{a,c} Therefore, the NRC staff requested Westinghouse perform a sensitivity analysis to determine the model's predictive uncertainty in RAI-SNPB-23. In response to RAI-SNPB-23, Westinghouse **[**

]^{a,c}

[

][a,c]

Because Westinghouse performed a sensitivity which demonstrated that the model's predictions were relatively independent of the data being predicted (i.e., training data or validation data), the NRC staff has determined that this goal has been met.

3.1.3.4.2 Statistical Method

Statistical Method
The validation error statistics should be calculated using an appropriate method.
G3.4.2, Review Framework for Critical Boiling Transition Models

In the initial submittal, Westinghouse calculated **[**

][a,c] Westinghouse stated that the negative bias will not be credited but did not discuss how not crediting the negative bias is conservative. In response to RAI-SNPB-30, Westinghouse clarified that a negative bias implies the D5 model predicts a CP which is actually lower than the measured values, which is conservative. Westinghouse chose to ignore this negative bias and treat it as a conservatism. The NRC staff agrees that Westinghouse is being conservative by ignoring this negative bias.

The NRC staff was uncertain about the number of degrees of freedom Westinghouse was using in the analysis. Therefore, in response to RAI-SNPB-32, Westinghouse provided the degrees of freedom used in the analysis. The NRC staff found this number reasonable as it was consistent with the general method applied for calculating the degrees of freedom. Finally, Figure 6-7 from the initial submittal the NRC staff determined that the validation error **[** **]**[a,c]

Because the number of degrees of freedom has been correctly calculated, and the mean and standard deviation have been correctly calculated from the valuation error data set, the NRC staff has determined that this goal has been met.

3.1.3.4.3 Appropriate Bias for Model Uncertainty

Appropriate Bias
The model's error should be appropriately biased in generating the model uncertainty.
G3.4.3, Review Framework for Critical Boiling Transition Models

In the initial submittal, Westinghouse discussed two conservative biases applied to increase the model's uncertainty. First, the negative bias on the model's mean was ignored. Second, **[**

][a,c] This was the result of analyzing certain data points which were excluded from the process of training and validating the CPR model but were conservatively considered in the final D5 model uncertainty.

Because Westinghouse has biased the D5 model's uncertainties to be greater than the supporting validation error database, the NRC staff has determined that this goal has been met.

3.1.3.5 Model Implementation

The fourth sub-goal in demonstrating that the model's validation was appropriate is to demonstrate that the model will be implemented in a manner consistent with its validation. This is typically demonstrated using the two sub-goals as given in Figure **13** below.

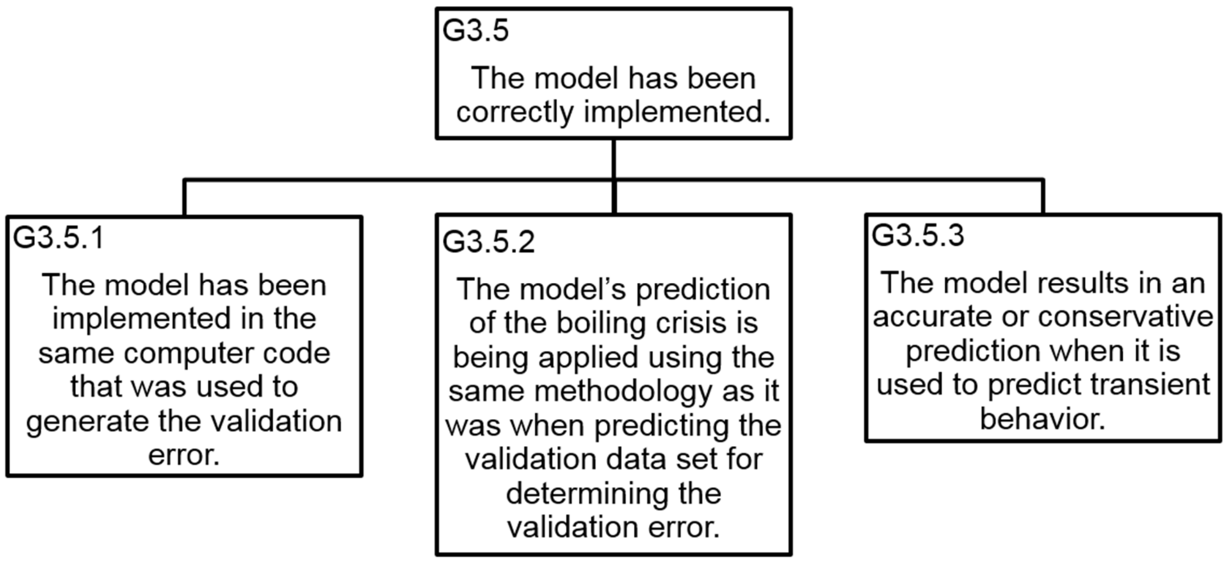

Figure 13: Decomposing G3.5 – Model Implementation

No further decompositions of the sub-goals were deemed useful. Therefore, the evidence demonstrating the following goals were met are provided below.

3.1.3.5.1 Same Computer Code

Same Computer Code

The model has been implemented in the same computer code which was used to generate the validation error.

G3.5.1, Review Framework for Critical Boiling Transition Models

In response to RAI-SNPB-34, Westinghouse identified that the D5 model will be implemented in BISON-SLAVE, as well as POLCA7, POLCA-T, GOBLIN, and BISON. They added that CPR models are independent of the thermal-hydraulics used in a steady-state code as they rely on thermal equilibrium. Additionally, in application in a transient computer codes, the code is validated against the FRIGG database of transient tests.

Because CP models do not rely on subchannel methods which are computer code specific and because the transient implementation of D5 will be validated against the transient tests, the NRC staff has determined that this goal has been met.

3.1.3.5.2 Same Evaluation Framework

Same Evaluation Framework

The model's prediction of the critical boiling transition is being applied using the same methodology as it was when predicting the validation error set for determining the model's error.

G3.5.2, Review Framework for Critical Boiling Transition Models

Unlike DNB models which are calculated in a subchannel code which has a number of complex closure relations, the application of a CPR model is relatively simple. A single channel is modeled with R-factors accounting for radial powers and additive constants accounting for thermal hydraulic effects. Given the simplicity of CPR models and Westinghouse's description of the procedures for implementation and validating such a model in a new computer code (response to RAI-SNPB-34), the NRC staff has determined that this goal has been met.

3.1.3.5.3 Transient Prediction

Transient Prediction

The model results in an accurate or conservative prediction when it is used to predict transient behavior.

G3.5.3, Review Framework for Critical Boiling Transition Models

In the initial submittal in Section 7, Westinghouse discussed the application of D5 in transient applications. To demonstrate the appropriateness of this application, Westinghouse performed transient dryout tests using each of the axial power shapes. These tests included power increase, flow reduction, and a combination of power increase and flow reduction transients. In response to RAI-SNPB-33, Westinghouse added that these tests were designed to bound the limiting transients in all reactor types for which SVEA-96 Optima3 fuel would be used. While a fast pressure increase cannot be performed due to test equipment limitations, the consequences of that increase on power and flow can be simulated in the test loop.

[

][a,c] In the supplemental response to RAI-SNPB-33, Westinghouse stated that the limiting ~~trainsets~~ transients were modeled using Westinghouse's BISON code (a time domain BWR dynamic code use for analyzing operational and safety related transients) and the forcing functions used in the FRIGG tests were chosen based on that simulated data.

In total, **[ ]**[a,c] tests were simulated with BISON, where the criterion for dryout was a maximum temperature change of **[ ]**[a,c] Figures 7-10 through 7-12 of the TR provide the comparison between the measured and predicted CPs. **[**

][a,c]

[

]a,c Because Westinghouse demonstrated that the D5 model was able to conservatively predict the transient behavior and that those transients were representative of the limiting AOOs which could be expected on ~~SVEA96~~ SVEA-96 Optima 3 fuel, the NRC staff has determined that this goal has been met.

3.2 Single fuel rod failure and multiple v-shaped marks at Leibstadt NPP

In 2015, the NRC staff became aware of operating experience from the Leibstadt NPP, in which steady-state dryout was believed to have occurred and resulted in a fuel failure. The failure occurred in a SVEA-96 Optima2 fuel assembly, which is very similar design to the Optima3 fuel assembly and uses a correlation that is very similar to D5. Because dryout is supposed to be prevented by the minimum CPR (MCPR) safety and operating limits, the NRC staff evaluated this operating experience to determine if there were underlying issues with the CP correlation and/or the fuel design in use at Leibstadt NPP that could affect the acceptability of the D5 correlation.

3.2.1 Description of Circumstances

3.2.1.1 Initial Discovery of a Failed Fuel Rod

On July 5, 2014, towards the end of Cycle 30, reactor power at Leibstadt NPP was decreased from 100 percent to 80 percent in anticipation of a planned rod pattern adjustment and control rod integrity test. Due to operator error, after the reactor had successfully been powered down to 80 percent, the control system attempted to bring the reactor back to 100 percent power by quickly opening the recirculation system flow control valves. The resulting increase in flow collapsed steam voids in the core, leading to an increase in neutron flux. The measured neutron flux quickly reached 118 percent, resulting in an automatic reactor scram. During the transient, the maximum heat flux from the cladding to the coolant was believed to have only reached 87 percent of its rated value at full power. Plant operators subsequently restarted the reactor. Seven days after the reactor scram, on July 12, 2014, an increase in inert gas activity was detected consistent with fuel rod damage. The control cell containing the affected bundle was located and ~~its~~ the power in a neighboring cell was suppressed with a control blade. The plant then continued operation until shutting down for a planned outage on August 11, 2014.

During the outage following Cycle 30, the affected fuel bundle was identified. Inspection of this fuel bundle found substantial localized oxidation of the zirconium cladding surrounding a cladding perforation on one rod, and a later inspection found what was believed to be increased localized oxidation on symmetric rod locations within the bundle. The affected bundle was not reloaded into the core when the plant was restarted for Cycle 31. Given the oxidation and the shape of the markings, it was initially assumed that dryout had occurred. However, the fuel assembly in question should have had substantial margin to dryout during normal operation
[ ]a,c

3.2.1.2 Observations Following Cycle 31

Cycle 31 was completed on August 10, 2015, with no fuel failures. During the outage following Cycle 31, the fuel bundle in the same core location as the bundle containing the leaking fuel rod in Cycle 30 was visually inspected. Though the cladding was intact, V-shaped discolored areas on the cladding surface were found on the upper portion of some fuel rods. The markings were initially believed to be caused by locally enhanced oxidation, which was attributed to an increase in cladding temperatures caused by the dryout of the liquid film flowing along the fuel cladding. This finding spurred further visual inspections, which revealed some additional fuel rods which had V-shaped marks located in bundles throughout the core.

When these inspections were completed, the plant restarted for Cycle 32, voluntarily increasing the MCPR operating limit to 1.45 to provide additional margin against dryout. Because the root cause analysis to explain the apparent dryout indications was still underway, the Swiss Federal Nuclear Safety Inspectorate (ENSI) mandated this higher operating limit be maintained throughout the cycle. **[**

]^{a,c}

3.2.1.3 Observations Following Cycle 32 and Extended Inspection Campaign

Cycle 32 was completed on August 2, 2016, with no fuel failures. However, inspections performed during the outage following Cycle 32 again revealed V-shaped marks on certain fuel rods. Compared to Cycle 31, the number of V-shaped marks increased in Cycle 32, which was unexpected given the extra measures taken to add margin to the CPR limit. The inspection program was therefore expanded to include a total of more than 200 fuel bundles, and the plant's outage was extended while fuel inspections were carried out.

After the inspection campaign was completed, the plant was authorized by ENSI to restart on February 16, 2017, subject to limiting the core flow rate to below 95 percent and limiting the power of fresh fuel bundles to below 7.0 megawatts (or 7.2 megawatts for short periods of time). This effectively limited the core power to 95 percent at beginning of cycle and 88 percent at end of cycle.

Leibstadt NPP also committed to extended fuel assembly inspections in the future to confirm the adequacy of corrective actions to address the issue.

Fuel inspections following completion of Cycle 33 (2017) and Cycle 34 (2018) found no new V-shaped marks. In 2019, KKL has was given permission for a 2 percent power increase, but not for an increase in flow rate.

3.2.1.4 Post-Irradiation Examinations

Following Cycle 32, a number of fuel rods with V-shaped marks were subjected to further examination. In total, there were 205 visual inspections of fuel assemblies, **[ ]**[a,c] pool side inspections using the Frequency Scanning Eddy Current Technique (FSECT), and three rods sent for hot cell examinations at the Paul Scherrer Institute. The rods sent for hot cell inspection included **[**

][a,c]

[

][a,c]

[

][a,c]

Hot cell examinations and poolside measurements revealed that the vast majority of the observed V-shaped marks were not the result of excessive cladding oxidation, but instead were localized crud deposits. The crud was zinc-based (mainly ZnO and Zn_2SiO_4) and believed to be deposited by the repeated formation of dry patches or near dry patches (i.e., localized dryout/rewet of the coolant film). The crud was very water soluble and, as a result, crud could only be deposited in a region if the adjacent water film had a very high concentration of the chemical compounds present in the crud. While the crud could have been deposited when a dry patch formed, it could also have resulted from a thinning of the liquid film on the surface to a point that would allow the chemical compounds to be concentrated enough to come out of solution (without complete dryout). Given that there was some increase in oxidation for some of the fuel rods, dry patches must have formed on these rods at some point, and possibly many times[3]. Because only a small quantity of crud could be deposited during a single evaporation or near evaporation of the thin film, the same rod would have to experience multiple evaporation and rewet cycles to deposit the amount of crud observed from the hot cell testing.

The hot cell testing along with FSECT measurements provided insights into the maximum temperatures that were likely obtained in the fuel. During normal operation, radiation damage progressively increases the hardness of the cladding and the cladding liner. The hardness saturates in about 6 months (Ref. 21). While the plant operates at temperatures around 325°C, the hardness due to radiation damage will begin to recover (i.e., the cladding will anneal) if the

---

[2] **[**

][a,c]

[3] For cases in which oxidation did not increase, it is not possible to distinguish between if a fuel rod experienced a dry patch (complete dryout of the water film which deposited crud) or a near dry patch (extreme thinning of the water film allowing which deposited crud). Therefore, the term dry patch will be used for both instances.

cladding temperature reaches close to 400°C. The amount of hardness recovery is proportional to the temperature as well as the time the cladding spends at that temperature. Thus, hardness recovery can be used to estimate the maximum temperature experienced by the cladding and provide insights into the duration of the event.

Both the neighbor to the failed rod and the rod with the strong V-shaped mark were analyzed to determine the amount of hardness recovery. The neighbor to the failed rod had approximately a **[ ]^{a,c}** hardness recovery in both the cladding surface and the liner. Achieving a **[ ]^{a,c}** hardness recovery would mean that the rod experienced either hours of operation at temperatures close to **[ ]^{a,c}** or only a few minutes or seconds of operation at temperatures close to **[ ]^{a,c}** If the rod experienced longer operation at higher temperatures, the amount of hardness recovery would have been greater. Therefore, this hardness recovery effectively demonstrates that the neighbor to the failed rod did not experience temperatures in excess of 500°C.

The rod with the strong V-shaped mark had a **[ ]^{a,c}** hardness recovery in the cladding surface and no discernable recovery in the liner. Again, this hardness recovery effectively demonstrates that strong V-shaped mark rod did not experience temperatures in excess of 400° C.

The maximum temperature experienced by the analyzed fuel rods is also corroborated by the FSECT oxidation measurements. The neighbor rod had a zirconium oxide layer of **[ ]^{a,c}** which corresponds to some additional oxidation over a reference oxide thickness of **[ ]^{a,c}** and therefore appears to have experienced some heat up. On the other hand, the rod with the strong V-shaped mark had a zirconium oxide layer of **[ ]^{a,c}** which is within the expected zirconium oxide thickness range and therefore would have experienced at most a small temperature increase.

3.2.1.5 Summary of Inspection and Analysis

Visual inspections were performed on SVEA-96 Optima2 fuel assemblies that were first inserted in Leibstadt NPP as early as Cycle 22. Though only a limited number of assemblies were inspected prior to Cycle 30, the inspections found V-shaped marks of the type connected to the Cycle 30 fuel rod failure beginning in Cycle 28. Of the 200 bundles inspected, 47 had rods with V-shaped markings and one rod was found to have failed.

All the marks found during the visual inspection were of the same wedge shape, with length varying from a few millimeters up to a significant portion of the span between the spacer grids. All the marks were found near the top of the assembly (below the 7th and/or 8th spacer grid, which are the top two in the assembly), on the rods adjacent to the part-length rod in the corner of the bundle. All the marks had approximately the same azimuthal orientation, facing halfway between the channel wall and the corner rod position.

Marks were only observed on bundles above two types of inlet orifice positions, side-entry orifice (SEO) position type 3 and SEO position type 2. As shown in Westinghouse's RAI response (Ref. 20), about 40 percent of the inspected SEO-3 bundles were found to have the V-shaped marks, while only 12 percent of the SEO-2 and none of the SEO-1 bundles had marks. It is worth noting that significantly fewer SEO-1 bundles were inspected than SEO-2 or SEO-3, but the staff performed a statistical analysis that found that the number of SEO-1 bundles inspected should have been sufficient to uncover affected bundles if the population of SEO-1 bundles was consistent with the population of SEO-2 or SEO-3 bundles.

As discussed in Section 3.2.1.4 above, the V-shaped marks were found to be composed of a zinc-rich crud that was very water soluble. Tests on the cladding and liner hardness carried out during the hot cell examinations concluded that even the most affected rods likely did not experience cladding temperatures in excess of 500°C (932°F).

Based on the operating characteristics of the Leibstadt NPP plant and core, the characteristics of the SVEA-96 Optima2 fuel, and the characteristics of the zinc-rich crud layer, the NRC staff concluded that the markings were probably created during the fuel's first cycle of operation, and likely towards the end of the cycle. The affected bundles were all operated at bundle powers of greater than 7.4 megawatts over the period during which the marks are believed to have been created. However, the affected bundles also had significant steady-state MCPR margin in their first cycle of operation, with a minimum CPR of 1.38 among affected bundles. In the cycles in which the marks are believed to have been created, the core flow was maintained above 97 percent for an extended period near the end of the cycle.

3.2.2 Evaluation

Though the inspections discussed above were carried out as the result of the failure of a fuel rod during Cycle 30 at Leibstadt NPP, the inspections uncovered very little about the ultimate cause of this failure, which is not definitively known. Inspections of numerous other rods apparently affected by the same phenomena found, as discussed above, at most limited degradation that remained well within Swiss regulatory limits.

V-shaped marks of the type observed at Leibstadt NPP were only found on SVEA-96 Optima2 fuel, of which full cores have been loaded at Leibstadt NPP since Cycle 28. Westinghouse has inspected **[ ]**^{a,c} Optima2 assemblies from **[ ]**^{a,c} other BWRs, including another BWR/6, and found no other similar marks. In total, over 12,000 Optima2 assemblies have been operated, many of which operated at lower CPRs than the assembly in which the fuel rod failure occurred, with no failures or other indication of dryout.

To determine the underlying phenomena that caused the fuel rod failure and dry patches at Leibstadt NPP, Westinghouse conducted a root cause investigation into the V-shaped marks observed at Leibstadt NPP, which concluded that the marks were the result of dry patches that formed due to the combined effect of bi-stable recirculation loop flow and the formation and dissipation of vortices at fuel assembly inlet orifices.

Over the course of this review, the NRC staff focused on three of those potential root causes which it considered to be the most significant. The first root cause considered was that dryout had occurred and the D5 CPR model had not predicted the margin correctly. The NRC also considered that an unanalyzed intra-bundle instability had occurred between the subchannels in the fuel bundle. The final root cause considered was that the dry patches were the result of local flow disturbances caused by vortex dispersal and reformation in front of SEO positions which itself was aggravated by high frequency bi-stable flow; this is consistent with the root cause proposed by Westinghouse. These root causes are all evaluated in the following sections.

3.2.2.1 Possibility of Error in D5 CPR Model

The NRC staff is aware of two previous events in which dryout occurred during operation of a NPP. In 1988 at Oskarshamn 2 (Ref. 27), one corner rod had failed in each of four fuel

assemblies. The root cause was found to be excessive channel bow caused by re-used fuel channels, which resulted in increased water gaps and much higher corner rod peaking powers than expected. In Forsmark 2 (Refs. 19 and 25), a lightning strike resulted in tripping the main recirculation pumps, which caused a rapid decrease in core flow and resulted in 18 assemblies experiencing a CPR ratio below 1.0 (i.e., they were predicted to experience a CBT). Given the short length of the transient (less than 1 second), the peak cladding temperatures from dryout were estimated to at most 450 °C. This estimation was made through data from hot cell inspections. All the affected fuel assemblies at Forsmark were verified to satisfy the requirements for continued operation and were later reloaded into the reactor. In both instances, the occurrence of dryout was consistent with analytical predictions, after accounting for the changes that occurred to reactor operating parameters during the events.

While reviewing the D5 CPR model, the NRC staff considered the possibility that the V-marks observed at Leibstadt NPP were due to dryout, and therefore there was an error in the applicable CPR model (which had predicted ample margin to dryout). This error could have been in the model itself (i.e., that it did not correctly reproduce the empirical data which was used to generate the model) or the error could have been in the data (i.e., the model did reproduce its underlying empirical data, but that data was itself in error). The NRC staff first considered the potential for a mathematical error in the model and were able to quickly discount this possibility, as the predictions of the D5 model matched very closely with test points which were near to the conditions at which the single fuel failure occurred. Both the model and the test data showed substantial margin to dryout.

Next, the NRC staff considered the possibility that the experimental data which was used to generate the D5 model could be a poor representation of the actual CP performance of the Optima assembly. The credibility of the test facility is specifically addressed above in Goal 1.1, discussed in Section 3.1.1.1, "Credible test facility." The discussion related to Goal 1.1.2 in Section 3.1.1.1.2, "Test facility comparison," provided benchmarks for the FRIGG loop against another test facility, which demonstrated that the two facilities produced very similar results. The NRC staff also visited the test facility where the data was taken, to better understand the test facility design and procedures. As discussed in these assessments in the SE, the NRC staff found the test facility to be credible. While these assessments cannot rule out the possibility that there could be a difference in phenomena occurring in the test assembly compared to those occurring in the reactor, it did confirm that the Westinghouse CPR test data was generated in a manner consistent with the NRC staff's expectations.

As more inspection data became available following Cycle 32, the NRC staff increasingly believed an error was unlikely in the D5 model and supporting testing data. The CPR models are used to predict the dryout of a thin annular film on the fuel rod surface. While the CP behavior of each fuel design is different, there are several similarities typical of all fuel designs and CP correlations. One such similarity is that increasing the flow of water through the core will increase the margin to dryout. Therefore, it is common to address a CPR penalty, such as the penalty applied to Leibstadt NPP in Cycle 32, by increasing the mass flow rate in the core. **[**

][a,c] This behavior would not be expected if these dry patches were caused by the dryout of a thin film.

Additionally, the realization that the V-marks were mostly crud, as opposed to zirconium oxide, meant that the dry patches had to repeatedly form and quickly rewet, so the zinc-rich crud could be deposited without a significant increase in the cladding surface temperature. The inspection data suggests that there was sufficient water near the rod to maintain temperatures relatively

close to operating conditions. The NRC staff therefore found it reasonable to conclude that a transient effect was causing the annular film to thin or dry out completely.

One of the key pieces of evidence that the dry patches formed at Leibstadt NPP were not related to the CBT examined in CPR testing comes from the inspection data. The inspection data strongly suggests that the formation of a V-mark in a given assembly was statistically independent from that assembly's minimum CPR value. While the CPR model is used to calculate that margin, and the correctness of that model is being evaluated, it would be unlikely that an error in the CPR model would cause it to calculate purely random values of CPRs. However, the minimum CPR values from the assemblies in which V-marks had formed looked to be a random sample of all minimum CPR values in the entire core.

Because the experimental data which confirmed the CPR model's predictions of substantial margin to dryout in the reactor were taken at conditions very close to those experienced at Leibstadt NPP, because the experimental data were obtained from a credible test facility (which was benchmarked against CPR data from another facility), because the dry patches did not experience significant temperature increases, and because the dry patches were uncorrelated with the CPR value and known CPR behavior, the NRC staff concludes that there is reasonable assurance that the dry patches that formed at Leibstadt NPP did not result from an error in the D5 CPR model.

3.2.2.1 Intra Bundle Instability

The NRC staff also considered a root cause in which the V-marks were linked to intra-bundle instability. After consideration, the NRC staff concluded that an intra-bundle instability was unlikely the root cause of the dry patch formation due to the following reasons:

1) The SVEA design has been tested on multiple occasions and has been demonstrated to have increased thermal-hydraulic stability compared to an open lattice design. The increased stability of the design has been confirmed during operation. Additionally, Westinghouse has performed testing and analysis which specifically considered parallel channel instability and concluded that the lateral communication through the slots between each sub-bundle is more than sufficient to prevent parallel channel instability (Ref. 20).
2) Instability would be most likely at the beginning of the cycle. Any V-marks formed at the beginning of the cycle would likely have mostly dissipated by the end of the cycle due to the solubility of the crud. However, the observation of many distinct V-marks strongly suggests that the marks were formed toward the end of the cycle.
3) When the operating procedures were changed in Cycles 33 and 34 to eliminate the observed issues, the changes had little effect on behavior at the beginning of the cycle. However, the reduction in power and flow, particularly towards the end of the cycle, resulted in a complete cessation of the V-marks.
4) If an intra-bundle instability was occurring, some fuel bundles in their second cycle of operation should have been more susceptible, as they operated at higher powers during the beginning of the second cycle. However, this is not supported by the data. V-marks were not observed to have formed in any second cycle assembly.

3.2.2.2 Westinghouse's Proposed Root Cause

Westinghouse's root cause theorized that the V-marks at Leibstadt NPP were not occurring in the thin film annular flow region, but in a thick film annular flow region. This would be consistent with the predicted CPR values, as the annular film would be expected to have a thick film at the values predicted by the D5 model. Because annular flow in the thick film region behaves differently than annular flow in the thin film region, this theory would explain why the V-marks displayed behavior and sensitivities inconsistent with the dryout behavior of thin films. While thick film annular flow has been previously studied, it is generally not focused on in the review of a CPR model, and further, the CPR model is not trained on data in the thick film region. Instead, CPR models are trained to predict stable film dryout which occurs in the thin film region.

Dry patches caused by step changes in flow

The thin film region of annular flow is characterized by a very thin water film surrounding the fuel rods. While the thin film is carried up the rod by the vapor in the core of the channel, the film is too thin to support surface waves. The main phenomena which impact the film thickness are evaporation, which reduces the film thickness; deposition of water droplets from the channel onto the film, which increases the film thickness; and entrainment of water from the film into the channel, which decreases the film thickness. The heat transfer from evaporation is so high that the wall temperature under the film is unable to attain the necessary amount of superheat needed to cause boiling (i.e., nucleation).

The thick film region of annular flow is characterized by a thick water film surrounding the fuel rods. The thick film is carried up the rod by the vapor in the core of the channel, but the film is thick enough to support surface waves. Moreover, most of the water in the film exists in the crests of those waves, and therefore there is less water in the troughs between the waves. Given the large margins to CPR predicted by the D5 model for the thin annular film region, it is reasonable to infer that the V-shaped marks would have formed in the thick annular film flow regime. Westinghouse proposed that a step change in local flow conditions could cause a momentary interruption to the waves carrying the water. The interruption could result in dry patch formation until the change in flow conditions equalized and the surface waves started again at a new steady state. The NRC staff finds that Westinghouse's explanation accounts for many of the inspection results. The proposed phenomena explain why the V-shaped marks formed at conditions far from dryout and why the cladding temperature did not experience significant heat up, as the dry patch would have been relatively quickly rewet.

Data from experiments confirmed that step changes in local conditions can create momentary transients which interrupt the waves that replenish the water on the fuel rod surface. One experiment (Ref. 32) showed that this interruption resulted in a coolant film disruption and led to a brief dry patch formation. Once the new steady state of wave production was reached, the waves replenished the water along the surface and the dry patch was rewet. **[**

][a,c]

Further, the impact of these transients would be expected to be the greatest in regions of the fuel bundle which had the highest vapor flow, as these regions would likely be subject to the largest vapor velocity changes during such a transient. The regions in which the dry patches

were observed (above the 1/3 part-length rods) **[**
]a,c

The NRC staff concluded based on a review of the experiments discussed above that step changes in the local flow conditions could momentarily disrupt a thick annular film, and that such a disruption would produce dry patches with the characteristics observed at Leibstadt NPP. Next, the NRC staff considered Westinghouse's explanation of what could cause such step changes to occur.

<u>Step changes in flow caused by vortex formation and dispersal</u>

Early in the inspection process, it became apparent that the V-marks were strongly correlated to the SEO position. While V-marks were also observed in some SEO-2 positions, it was with much less frequency than V-marks observed in SEO-3 positions. V-marks were never observed in SEO-1 positions. This strong correlation to SEO position suggested that the V-mark formation could be related to another phenomenon which was also correlated to SEO position.

In 2002, the General Electric Company (GE) submitted a Part 21 notification to the NRC (Ref. 33) discussing the need to adjust the SEO loss coefficients due to the core support structure, as bundles adjacent to zero core support beams (SEO-1), one core support beam (SEO-2), or two core support beams (SEO-3), as these bundles had loss coefficients which were too low. SEO-2 positions should have had a loss coefficient about 20 percent higher than SEO-1 positions, and SEO-3 positions should have had a loss coefficient about 40 percent higher than SEO-1 positions. The overall impact of this correction to the CPR margin was approximated to be 0.01. This represented a very minor impact, but it was accounted for BWR/6 CPR values.

[

]a,c

The NRC staff concluded based on a review of the experiments, analysis, and operation data discussed above that there are likely vortices which exist in the lower plenum next to SEO positions, that these vortices seem to have the most impact on SEO-3 positions, and these vortices would cause the step change in local flow conditions should the vortices suddenly form or dissipate. However, the presence of vortices alone would not cause step changes in local flow conditions. Therefore next, the NRC staff considered Westinghouse's explanation of what could cause the vortices to form and dissipate, resulting in a step change of flow conditions.

<u>Vortex formation and dissipation caused by bi-stable flow</u>

Based on experimental data, computational analysis, and plant data, Westinghouse postulated that vortices would form in the lower plenum of a BWR/6 under normal conditions, but that they could be dispersed by strong crossflows. Westinghouse further postulated that strong crossflows in the lower plenum were generated at Leibstadt NPP during the affected cycles by bi-stable flow conditions in the recirculation loops. Bi-stable flow is a phenomenon that is documented to occur in some BWRs (Refs. 29 and 30). It is related to the design of the

recirculation system and occurs when the recirculation loop flow oscillates between two stable modes. **[**

][a,c]

Westinghouse believed that following a vortex dissipation caused by a bi-stable flow transition, the vortex would re-form (potentially in a different structure) with the resumption of a stable flow pattern in the lower plenum. They hypothesize that vortex dissipation and reformation would cause a sudden change in bundle flow conditions, which would then result in the temporary disruption of the waves in the annular film region where the dry patches were postulated to occur. **[**

][a,c]

The NRC staff concluded based on a review of the plant data, that bi-stable flow conditions at Leibstadt NPP could cause vortices to form and dissipate, that these conditions were prevalent when in cycles where V-shaped marks were observed, that when these conditions were avoided in later cycles V-shaped marks were no longer observed, and that **[**

][a,c]

<u>Summary</u>

In summary, the NRC staff concluded that Westinghouse's root cause provided a phenomenological explanation of the formation of the V-shaped marks and is supported by inspection data, experimental data, and computational analysis. The root cause explains why the V-shaped marks were determined to have formed at the end of the cycle, how the V-shape marks could form and rewet intermittently and repeatedly allowing crud to build up, and why fuel rod surface temperatures remained relatively low. The root cause explains why SEO-3 positions would be the most susceptible and what **[**

][a,c] Finally, the root cause explains why the V-shaped marks were observed in certain cycles and not observed in other cycles.

---

[4] **[**

][a,c]

3.2.3 Conclusion

Based on the information collected on the phenomenon and operating conditions under which it was experienced, the NRC staff finds that there is sufficient evidence to conclude that bi-stable flow in the recirculation loops of a plant with lower plenum cross beams is a necessary precursor to the cladding degradation mechanism observed at Leibstadt NPP. This finding is based on the strong link between SEO-3 positions and V-marks (and the absence of SEO-3 positions in BWRs without lower plenum cross beams), and the strong link between proximity to the main jet pump riser focal points and the discovery of cladding degradation. While the NRC staff believes that the description of phenomena linking bi-stable flow to fuel damage (i.e., lower plenum vortex formation and dissipation and resulting pressure waves stripping the thick film from the cladding) is compelling, the NRC staff did not believe it was necessary to make a formal finding on the root cause analysis regarding D5.

Thus, the NRC staff finds that there is reasonable assurance of adequate protection in the application of the D5 CPR model to predict the CP performance of SVEA-96 Optima3 fuel to demonstrate compliance with GDC 10, subject to the following condition: when the D5 model is applied to Optima3 fuel in BWR/6 plants (or other plants with a similar lower plenum design which have cross beams in a grid formation in the lower plenum), the recirculation loops should be monitored for indications of bi-stable flow, and if necessary, corrective actions should be taken to avoid extended operation under these conditions. Licensees of BWR/6 plants proposing to load Optima3 fuel must establish limits on plant operation in a bi-stable flow condition that are sufficient to preclude this cladding degradation.

4.0 LIMITATIONS AND CONDITIONS

The following conditions must be true for the use of the D5 CPR model.

1. The D5 model is approved over the application domain specified in Table 6-7 of the TR.

2. Westinghouse will monitor the reload design process and ensure that sub-bundles with "high" R-factors have sufficiently large margins to the core minimum CPR (i.e., **[** **]**^{a,c} Further, they will quantify and include the impact of a **[** **]**^{a,c} should this margin not be maintained.

3. If it is likely that bundles with **[** **]**^{a,c} are either limiting or contributing to the SLMCPR bounding the cycle, those bundles shall have a bounding bias applied.

4. When the D5 model is applied to Optima3 fuel in BWR/6 plants (or other plants with a similar lower plenum design which have cross beams in a grid formation in the lower plenum), the recirculation loops shall be monitored for indications of bi-stable flow, and if necessary, corrective actions shall be taken to avoid extended operation under these conditions. Licensees of BWR/6 plants proposing to load Optima3 fuel must establish limits on plant operation in a bi-stable flow condition that are sufficient to preclude this cladding degradation.

5.0 CONCLUSION

Based on evidence provided in Section 3.1.1, "Experimental data," of this SE, the NRC staff concludes that the experimental data supporting the D5 model is appropriate. Based on the

evidence in Section 3.1.2, "Model generation," of this SE, the NRC staff concludes that D5 model was generated in a logical fashion. Based on the evidence in Section 3.1.3, "Model validation," of this SE, the NRC staff concludes that the D5 model has sufficient validation as demonstrated through appropriate quantification of its error. Therefore, based on the cumulative evidence, the NRC staff concludes that the D5 model is acceptable for use in reactor safety analysis subject to the limitations and conditions in Section 4.0 of this SE.

6.0 REFERENCES

1. Gresham, J.A., Westinghouse Electric Company, letter to U.S. Nuclear Regulatory Commission, "Submittal of WCAP-17794-P, Revision 0 and WCAP-17794-NP, Revision 0, '10xl0 SVEA Fuel Critical Power Experiments and New CPR Correlation: D5 for SVEA-96 Optima3' (Proprietary/Non-Proprietary)," LTR-13-76, November 22, 2013 (Agencywide Documents Access and Management System (ADAMS) Accession No. ML13333A274).

2. Bergmann, U., Hemlin, M., Bergman, K., and J-M. Le Core, Westinghouse Electric Company, "10xl0 SVEA Fuel Critical Power Experiments and New CPR Correlation: D5 for SVEA-96 Optima3", WCAP-17794-P/NP, Revision 0, November 2013 (ADAMS Accession Nos. ML13333A275 (*Non-Proprietary Version/Publicly Available* and ML13333A276 (*Proprietary Version/Non-Publicly Available*)).

3. Harris, W.R. and Y.Y. Yung, Combustion Engineering, "10x10 SVEA Fuel Critical Power Experiments and CPR Correlations: SVEA-96," CENPD-392-P-A, Revision 00, September 2000 (ADAMS Accession Nos. ML003767366 (*Non-Proprietary Version/Publicly Available*) and ML003767392 (*Proprietary Version/Non-Publicly Available*)).

4. Harris, W.R. and Y.Y. Yung, ABB Combustion Engineering Nuclear Power, Inc., "10x10 SVEA Fuel Critical Power Experiments and CPR Correlations: SVEA-96+," CENPD-389-P-A, September 1999, ADAMS Accession Nos. ML993420024 (*Non-Proprietary Version. Publicly Available*) and ML993470286 (*Proprietary Version/Non-Publicly Available*)).

5. Harris, W., Majed, M., Norback, G. and Y.Y. Yung, Westinghouse Electric Company, "10x10 SVEA Fuel Critical Power Experiments and CPR Correlation: SVEA-96 Optima2", WCAP-16081-P-A, March 2005, ADAMS Accession No. ML051260213 (*Proprietary Information/Non-Publicly Available*).

6. Mendiola, A.J., U.S. Nuclear Regulatory Commission, letter to J. A. Gresham, Westinghouse Electric Company, "Acceptance for review of Westinghouse Electric Company (Westinghouse) Topical Report WCAP-17794-P, Revision 0 and WCAP-17794-NP, Revision 0, '10x10 SVEA Fuel Critical Power Experiments and New CPR (critical power ratio) Correlations: D5 for SVEA-96 Optima3' (TAC NO. MF3368)," April 28, 2014 (ADAMS Accession No. ML14093A214).

7. Dean, J.L., U.S. Nuclear Regulatory Commission, memo to A.J. Mendiola, U.S. Nuclear Regulatory Commission, "Audit plan for Audit for Understanding on WCAP-17794 '10x10 SVEA Fuel Critical Power Experiments and new CPR correlation: D5 for SVEA-96 Optima3' (TAC NO. MF3368)," May 18, 2015 (ADAMS Accession No. ML15138A187 (*Non-Publicly Available)*).

8. Dean, J.L., U.S. Nuclear Regulatory Commission , memo to A.J. Mendiola, U.S. Nuclear Regulatory Commission, “Summary of Audit for Understanding Conducted Between June 3, 2015 and June 4, 2015 for WCAP-17794-P, ‘10x10 SVEA Fuel Critical Power Experiments And New Critical Power Ratio Correlation: D5 For Svea-96 Optima3’ (TAC No. MF1797),” June 18, 2015 (ADAMS Accession No. ML15167A276 (*Non-Publicly Available*)).

9. Gresham, J.A., Westinghouse Electric Company, letter to U.S. Nuclear Regulatory Commission, “Submittal of Data to Support NRC Review of WCAP-17794-P with Respect to the D5 Correlation for SVEA-96 Optima3 Fuel (Proprietary/Non-Proprietary)," LTR-15-52, June 22, 2015 (ADAMS Accession Nos. ML15176A967 (*Submittal Letter/Publicly Available*), ML15176A963 (*Non-Proprietary Attachment/Publicly Available*) and ML15176A965 (*Proprietary Attachment/Non-Publicly Available*)).

10. Lenning, K., NRC, letter to James Gresham, Westinghouse Electric Company, “Request for Additional Information Re: Westinghouse Electric Company Topical Report WCAP-17794-P, Revision 0 and WCAP-17794-NP, Revision 0, ‘10x10 SVEA Fuel Critical Power Experiments and New CPR Correlation: D5 for SVEA-96 Optima3’ (TAC No. MF3368,” May 31, 2016, ADAMS Accession No. ML16104A278 (*Submittal Letter/Publicly Available*), ML16104A281 (*Non-Proprietary Attachment/Publicly Available*), and ML16104A283 (*Proprietary Attachment/Non-Publicly Available*)).

11. Gresham, J.A., Westinghouse Electric Company, letter to U.S. Nuclear Regulatory Commission, “Responses to NRC Request for Additional Information for Westinghouse Electric Company Topical Report WCAP-17794-P/WCAP-17794-NP, Revision 0, ‘10x10 SVEA Fuel Critical Power Experiments and New CPR Correlation: D5 for SVEA-96 Optima3 Fuel (Proprietary/Non-Proprietary)," LTR-16-53, August 8, 2016 (ADAMS Accession No. ML16224B087 (*Submittal Letter/Publicly Available*), ML16224B088 (Non-Proprietary Attachment/Publicly Available), and ML16224B089 (*Proprietary Attachment/Non-Publicly Available*)).

12. Lenning, K., NRC, letter to James Gresham, Westinghouse Electric Company, “Request for Additional Information Re: Westinghouse Electric Company Topical Report WCAP-17794-P, Revision 0 and WCAP-17794-NP, Revision 0, ‘10x10 SVEA Fuel Critical Power Experiments and New CPR Correlation: D5 for SVEA-96 Optima3’ (TAC No. MF3368”, November 21, 2016 (ADAMS Accession No. ML16285A400).

13. Kaizer, J.S., NRC, Audit Plan, March 12, 2017 (ADAMS Accession No. ML17071A004) (*Proprietary Attachment/Non-Publicly Available*).

14. Gresham, J.A., Westinghouse Electric Company, letter to U.S. Nuclear Regulatory Commission, “Supporting Information for the NRC Audit of the D5 CPR Correlation (Proprietary/Non-Proprietary)," LTR-17-23, March 16, 2017 (ADAMS Accession Nos. ML17087A009 (*Submittal Letter/Publicly Available*), ML17087A010 (*Non-Proprietary Attachment/Publicly Available*), and ML17087A011 (*Proprietary Attachment/Non-Publicly Available*)).

15. Gresham, J.A., Westinghouse Electric Company, letter to U.S. Nuclear Regulatory Commission, “Submittal of Proprietary Westinghouse Information Presented at the NRC Audit for the D5 CPR Correlation (WCAP-17794-P) (Proprietary)," LTR-17-26, April 4, 2017 (ADAMS Accession No. ML17101A368 (*Submittal Letter/Publicly Available*) and ML17101A369 (*Proprietary Attachment/Non-Publicly Available*).

16. Gresham, J.A., Westinghouse Electric Company, letter to U.S. Nuclear Regulatory Commission, “Submittal of Proprietary Westinghouse Information Regarding the NRC Audit for the D5 CPR Correlation (WCAP-17794-P) (Proprietary)," LTR-17-13, April 13, 2017 (ADAMS Accession Nos. ML17115A422 (*Submittal Letter/Publicly Available*) and ML17115A423 (*Proprietary Attachment/Non-Publicly Available*)).

17. Lenning, K., NRC, letter to James Gresham, Westinghouse Electric Company, “Request for Additional Information RE: Westinghouse Electric Company Topical Report WCAP-17794-P, Revision 0, and WCAP-17794-NP, Revision 0, "10x10 SVEA Fuel Critical Power Experiments and New CPR Correlation: D5 for SVEA-96 Optima3" (TAC No. MF3368),” May 15, 2017 (ADAMS Accession Nos. ML17065A199 (*Submittal Letter/Publicly Available*), ML17065A204 (*Non-Proprietary Attachment/Publicly Available*), and ML17065A202 (*Proprietary Attachment/Non-Publicly Available*)).

18. Gresham, J.A., Westinghouse Electric Company, letter to U.S. Nuclear Regulatory Commission, “Responses to Supplemental Requests for Additional Information As Discussed During the NRC Audit of Westinghouse Topical Report WCAP-17794-P/ WCAP-17794-NP, Revision 0, "10x10 SVEA Fuel Critical Power Experiments and New CPR Correlation: D5 for SVEA-96 Optima3," LTR-17-45, June 12, 2017 (ADAMS Accession Nos. ML17170A123 (*Submittal Letter/Publicly Available*), ML17170A124 (Non-*Proprietary Attachment/Publicly Available*), and ML17170A125 (*Proprietary Attachment. Non-Publicly Available*)).

19. Gresham, J.A., Westinghouse Electric Company, letter to U.S. Nuclear Regulatory Commission, “Response to Revised November 21, 2016, U. S. Nuclear Regulatory Commission Request for Additional Information for Westinghouse Electric Company Topical Report WCAP-17794-P, Revision 0, and WCAP-17794-NP, Revision 0, "10x10 SVEA Fuel Critical Power Experiments and New CPR Correlation: D5 for SVEA-96 OPTIMA3" (Proprietary/Non-Proprietary)," LTR-17-77, December 18, 2017 (ADAMS Accession Nos. ML17354A043 (Non-*Proprietary Attachment/Publicly Available*) and ML17354A045 (*Proprietary Attachment/Non-Publicly Available*)).

20. Mercier, E.J., Westinghouse Electric Company, letter to U.S. Nuclear Regulatory Commission, “Fuel Failure Relevance to D5 and OPTIMA3 Topical Report Reviews (Attachment 1) and Updated Response to Revised November 21, 2016, U. S. Nuclear Regulatory Commission Request for Additional Information for Westinghouse Electric Company Topical Report WCAP-17794-P, Revision 0, and WCAP-17794-NP, Revision 0, “10x10 SVEA Fuel Critical Power Experiments and New CPR Correlation: D5 for SVEA-96 OPTIMA3” (Attachment 2) (Proprietary/Non-Proprietary)", LTR-18-51, July 16, 2018 (ADAMS Accession Nos. ML18198A201 (*Submittal Letter and* Non-*Proprietary Attachment/Publicly Available*) and ML18198A277 (*Proprietary Attachment/Non-Publicly Available*)).

21. Hosack, H.L., Westinghouse Electric Company, letter to U.S. Nuclear Regulatory Commission, “Proprietary Westinghouse Information Regarding the NRC Audit of WCAP-17794-P, "10x10 SVEA Fuel Critical Power Experiments and New CPR Correlation: D5 for SVEA-96 Optima3" (Proprietary)," LTR-18-87, December 19, 2018 (ADAMS Accession Nos. ML18354B194 (*Submittal Letter/Publicly Available*) and ML18354B199 (*Proprietary Attachment/Non-Publicly Available*).

22. Kaizer, J.S., Safety Evaluation on Topical Report-ANP-10341P, “The ORFEO-GAIA and ORFEO-NMGRID Critical Heat Flux Correlations,” September 24, 2018 (ADAMS Accession No. ML18214A480).

23. Anzalone, R., Safety Evaluation on Topical Report-ANP-10335P, Revision 0, “ACE/ATRIUM 11 Critical Power Correlation,” May 25, 2018 (ADAMS Accession No. ML18207A408)

24. Safety Evaluation on Topical Report-0116-21012, Revision 1, “NuScale Power Critical Heat Flux Correlations,” August 8, 2018 (ADAMS Accession No. ML18236A426).

25. Kaizer, J.S, “Identification of Non-Conservative Subregions in Empirical Models Demonstrated Using Critical Heat Flux Models”, *Nuclear Technology*, Vol. 190, 65-71, 2015.

26. Oberkampf, W.L and C.J. Roy. *Verification and Validation in Scientific Computing*. Cambridge University Press, Cambridge, 2010.

27. Becker, K.M., Engström, J., Nylund, O., Schölin, B., and B. Söderquist, “Analysis of the dryout incident in the Oskarshamn 2 boiling water reactor”, International Journal of Multiphase Flow, Volume 16, Issue 6, pp 959-974, November-December 1990.

28. Schrire, D., RamenBlad, E., Kese, W., and M. Nillson, “Transient Dryout in Forsmark2 during a fast pump runback – Verification of Peak Cladding Temperature,” Top Fuel, 2012.

29. Information Notice No.86-110: Anomalous Behavior of Recirculation Loop Flow in Jet Pump BWR Plants.

30. General Electric Nuclear Services Information Letter, “Recirculation System Bi-Stable Flow in Jet Pump BWRs,” SIL No. 467, July 28, 1988.

31. U.S. Nuclear Regulatory Commission Operations Center Event Report, “Fuel Support Side Entry Orifice Loss Coefficient in Core Monitoring System Databank,” October 4, 2002 (ADAMS Accession No. ML022820028).

32. Fukano, T., et al., “Fluctuation Characteristics of heating Surface Temperature Near an Obstacle in Transient Boiling Two-Phase Flow in a Vertical Annular Channel,” Nuclear Engineering and Design 219 (2003) 47-60.

33. Liquid films and droplet deposition in a BWR fuel element, PhD Thesis of Manuel Damsohn, Laboratory of Nuclear Energy Systems, Institute of Energy Technology, Department of Mechanical and Process Engineering, ETH Zurich, 2011.

34. Watanabe, S., Abe, Y., Kaneko, A., Watanage, F., Tezuka, K., and K. Hirao, "Effect of complicated coolant flow behavior in the ABWR lower plenum on flow distribution to the core," Nuclear Engineering and Design, 295, pp 1 – 14, 2015.

35. WCAP-15942-P-A, "Fuel Assembly Mechanical Design Methodology for Boiling Water Reactors, Supplement 1 to CENP-287," March 2006 (ADAMS Accession No. ML061110351 (*Proprietary/Non-Publicly Available*)).

7.0 LIST OF ACRONYMS

AOO	Anticipated Operational Occurrence
BWR	Boiling Water Reactor
CHF	Critical Heat Flux
CPR	Critical Power Ratio
CFR	Code of Federal Regulations
GDC	General Design Criteria
PWR	Pressurized Water Reactor
RAI	Request for Additional Information

Principal Contributors: J. Kaizer
R. Anzalone
J. Whitman

Date: July 17, 2019